

# The Athabasca Granulite Terrane and Evidence for Dynamic Behavior of Lower Continental Crust

Gregory Dumond,<sup>1</sup> Michael L. Williams,<sup>2</sup> and Sean P. Regan<sup>3</sup>

<sup>1</sup>Department of Geosciences, University of Arkansas, Fayetteville, Arkansas 72701, USA; email: gdumond@uark.edu

<sup>2</sup>Department of Geosciences, University of Massachusetts, Amherst, Massachusetts 01003, USA; email: mlnw@geo.umass.edu

<sup>3</sup>Center for Earth and Environmental Science, State University of New York, Plattsburgh, New York 12901, USA; email: sregan004@plattsburgh.edu

Annu. Rev. Earth Planet. Sci. 2018. 46:353–86

The *Annual Review of Earth and Planetary Sciences* is online at [earth.annualreviews.org](http://earth.annualreviews.org)

<https://doi.org/10.1146/annurev-earth-063016-020625>

Copyright © 2018 by Annual Reviews.  
All rights reserved



## ANNUAL REVIEWS Further

Click here to view this article's online features:

- Download figures as PPT slides
- Navigate linked references
- Download citations
- Explore related articles
- Search keywords

## Keywords

continental crust, garnet, granulite, lithosphere, melt, shear zone

## Abstract

Deeply exhumed granulite terranes have long been considered nonrepresentative of lower continental crust largely because their bulk compositions do not match the lower crustal xenolith record. A paradigm shift in our understanding of deep crust has since occurred with new evidence for a more felsic and compositionally heterogeneous lower crust than previously recognized. The >20,000-km<sup>2</sup> Athabasca granulite terrane locally provides a >700-Myr-old window into this type of lower crust, prior to being exhumed and uplifted to the surface between 1.9 and 1.7 Ga. We review over 20 years of research on this terrane with an emphasis on what these findings may tell us about the origin and behavior of lower continental crust, in general, in addition to placing constraints on the tectonic evolution of the western Canadian Shield between 2.6 and 1.7 Ga. The results reveal a dynamic lower continental crust that evolved compositionally and rheologically with time.

## INTRODUCTION

The origin, character, and evolution of lower continental crust remain intensely debated (Bürgmann & Dresen 2008, Rudnick & Gao 2014, Hacker et al. 2015). The debate persists because disparate data sets remain difficult to reconcile, e.g., geophysical observables (Ross et al. 2004, Bai et al. 2010, Copley et al. 2011, Schulte-Pelkum et al. 2017), xenolith data (Rudnick & Taylor 1987, Villaseca et al. 1999, Hacker et al. 2000, Mahan et al. 2012), and the record gleaned from deeply exhumed granulite terranes (Fountain & Salisbury 1981, Percival et al. 1992, Mahan et al. 2011). Conventional views of the lower continental crust have held that it is predominantly mafic (Rudnick 1992; Rudnick & Fountain 1995; Rudnick & Gao 2003, 2014). Recent work, however, suggests that heat flow and seismic velocity constraints can be satisfied by a range of end-member bulk compositions and that most lower continental crust need not be mafic (Figures 1 and 2) (Hacker et al. 2015). Lower continental crust in a variety of tectonic settings displays a range of seismic wavespeeds with P-wave velocities ( $V_P$ ) = 6.0–7.7 km/s (Hacker et al. 2015). Hacker et al. (2015) derived average  $V_P$  for four end-member lower crustal compositions that ranged from 6.8 to 7.2 km/s with densities of 2.9 to 3.2 g/cm<sup>3</sup>. These results are consistent with a compositionally heterogeneous lower continental crust and imply that some exhumed granulite terranes may be more representative of lower continental crust than previously thought.

We review more than 20 years of research on one of Earth's largest granulite terranes, the >20,000-km<sup>2</sup> Athabasca granulite terrane in the western Canadian Shield (Figures 3 and 4), and summarize evidence bearing on several important processes, including (a) compositional evolution of lower continental crust; (b) lower crustal densification, with implications for seismic velocity,

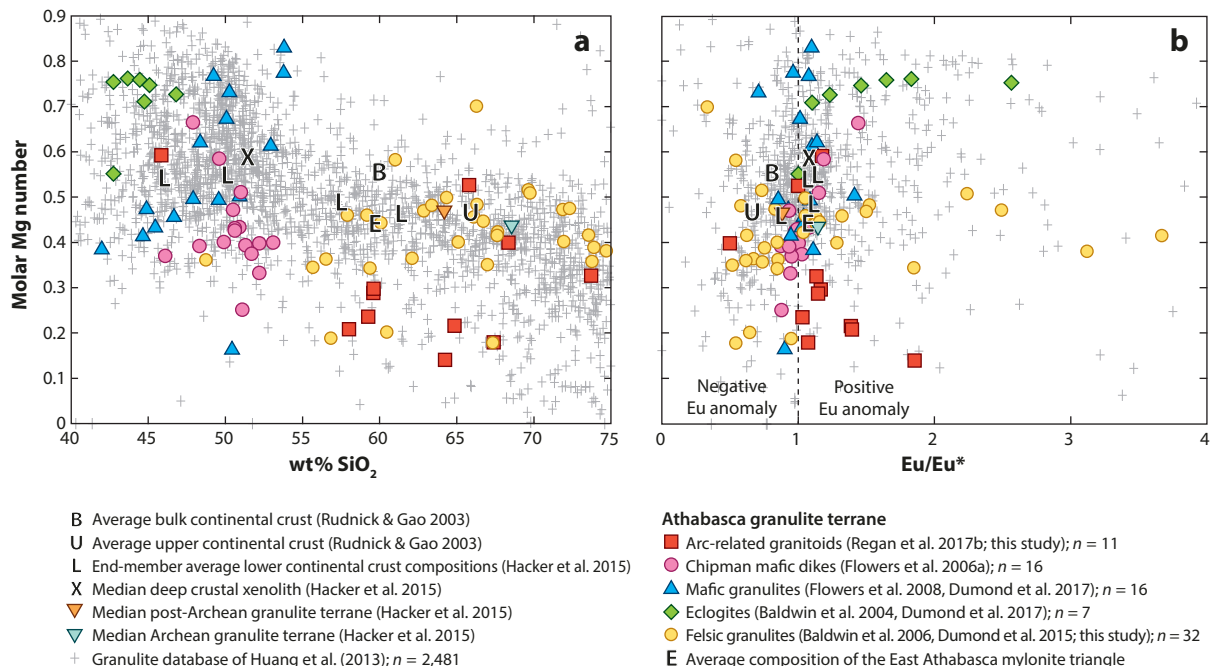


**Figure 1**

Bulk compositions from the Athabasca granulite terrane: (a) SiO<sub>2</sub> versus molar Mg number and (b) Eu/Eu\* (Eu anomaly) versus molar Mg number. The field of gray crosses corresponds to the granulite database of Rudnick & Presper (1990) that was updated by Huang et al. (2013).

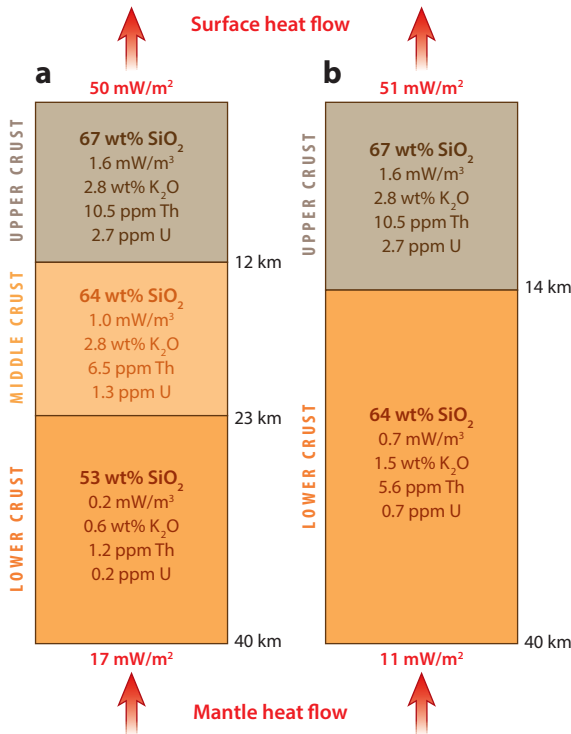


**Figure 2**

Continental crustal columns illustrating two end-members for the lower continental crust. (a) Three-layer model with mafic lower crust derived by Rudnick & Gao (2003, 2014). (b) Two-layer model with felsic lower crust derived by Hacker et al. (2011). Figure modified from Hacker et al. (2015) with permission.

crustal root growth, and foundering; (c) dynamic lower crustal rheology, with periods of weak flow and periods of high strength; and (d) mechanisms for stabilization and destabilization of continental lithosphere.

These processes affected the terrane at a range of timescales, with some portions of the terrane hypothesized to have experienced long-term (>650 Myr) lower crustal residence (Williams & Hanmer 2006, Flowers et al. 2008). This contrasts with other domains in the terrane that have been inferred to record short-term (10s to >100 Myr) residence in the deep crust (Martel et al. 2008, Bethune et al. 2013). This review begins with a summary of the geological record of the Athabasca granulite terrane, including hypotheses for the tectonic evolution of several domains within the terrane and their implications for the tectonic history of the western Canadian Shield (Figures 3 and 4). Observations from the Athabasca granulite terrane are then used to place constraints on the characteristics and evolution of deep continental crust in general.

## GEOLOGICAL BACKGROUND

The western Canadian Shield of North America consists of a number of Archean cratonic provinces, including the Churchill Province (Figure 3) (Hoffman 1988). The western extent of the Churchill Province is delimited by the Great Slave Lake shear zone and the 2.0–1.9 Ga Talson-Thelon orogen (Figure 3b) (Hoffman 1987, Ross 2002). The eastern boundary is marked by the 1.9–1.8 Ga Trans-Hudson orogen (Figure 3b) (Ansdel 2005, St-Onge et al.

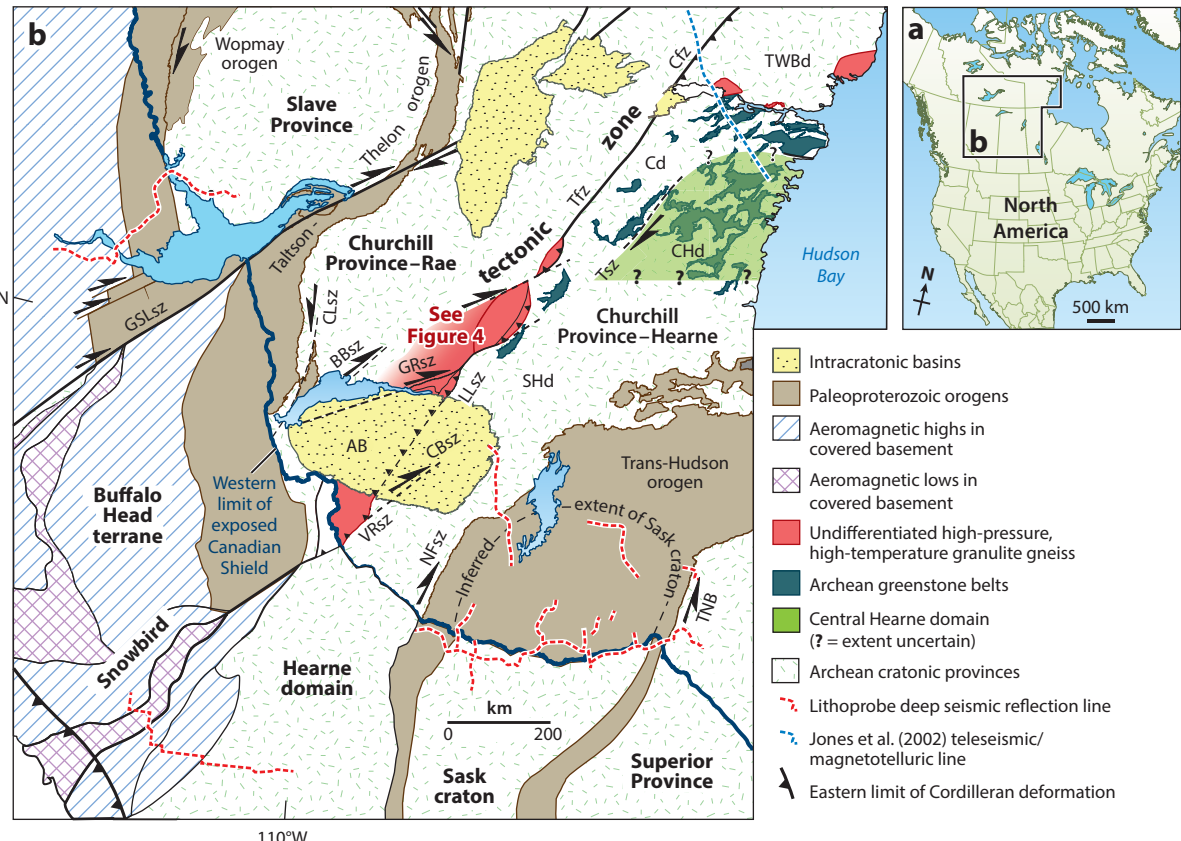


**Figure 3**

(a) Location of the western Canadian Shield in North America. (b) Simplified geologic map of the western Canadian Shield with data compiled from Hoffman (1988), Tella et al. (2000), Ross (2002), and Hajnal et al. (2005). Note location of **Figure 4** at center. Abbreviations: AB, Athabasca basin; BBsz, Black Bay shear zone; CBsz, Cable Bay shear zone; Cd, Chesterfield domain; Cfz, Chesterfield fault zone (Berman et al. 2007); CHd, central Hearne domain (Hanmer et al. 2004); CLsz, Charles Lake shear zone; GRsz, Grease River shear zone; GSLsz, Great Slave Lake shear zone; LLsz, Legs Lake shear zone; NFSz, Needle Falls shear zone; SHd, southern Hearne domain (van Breeman et al. 2007a); Tfz, Tulemalu fault zone; TNB, Thompson nickel belt; Tsz, Tyrell shear zone; TWBd, Tehery Wager Bay gneiss domain (van Breeman et al. 2007b); VRsz, Virgin River shear zone. Locations of Lithoprobe seismic reflection profiles are from <http://lithoprobe.eos.ubc.ca/transects/> (accessed December 14, 2017).

2006). Early geophysical studies subdivided the Churchill Province along a >2,800-km-long northeast-trending lineament defined by anomalies in the regional gravity and magnetic fields in Alberta, Saskatchewan, and the Northwest Territories (**Figure 3b**) (Walcott 1968, Wallis 1970, Walcott & Boyd 1971, Gibb et al. 1983). Hoffman (1988) first named the lineament the Snowbird tectonic zone, using it to define the boundary between the Rae and Hearne domains within the Churchill Province (**Figure 3b**). Portions of the Snowbird tectonic zone are associated with a discontinuous belt of high-pressure granulite (**Figure 3b**) (Tella & Eade 1986; Hanmer et al. 1994; Snoeyenbos et al. 1995; Williams et al. 1995, 2000; Hanmer & Williams 2001; Sanborn-Barrie et al. 2001; Baldwin et al. 2003, 2004, 2006, 2007, 2015; Mahan et al. 2003, 2006a,b, 2008, 2011; Mahan & Williams 2005; Williams & Hanmer 2006; Flowers et al. 2006a,b, 2008; Mills et al. 2007; Martel et al. 2008; Dumond et al. 2010, 2015; Regan et al. 2014, 2017a,b).

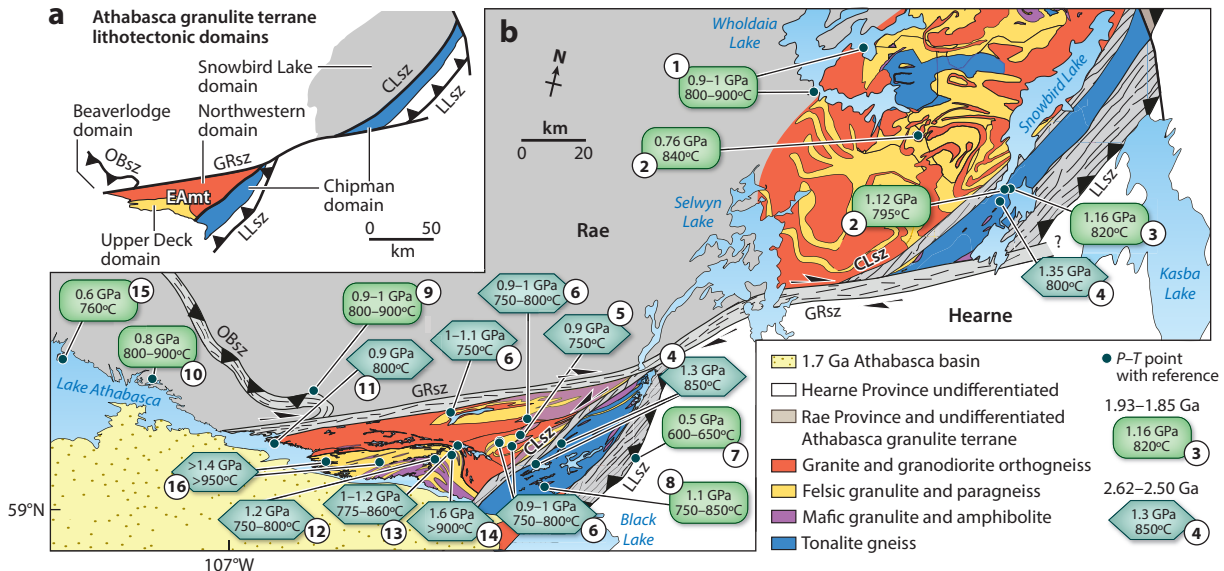


**Figure 4**

(a) Map of lithotectonic domains in the Athabasca granulite terrane discussed in the text. (b) Geologic map of the Athabasca granulite terrane with existing pressure–temperature–time ( $P$ – $T$ – $t$ ) data referenced by number: (1) Krikorian (2002); (2) Martel et al. (2008); (3) Mahan & Williams (2005); (4) Mahan et al. (2008); (5) Regan et al. (2014); (6) Williams et al. (2000); (7) Mahan et al. (2003); (8) Williams et al. (1995); (9) Williams & Hanmer (2006); (10) Kopf (1999) and Williams & Jercinovic (2002); (11) Dumond et al. (2010); (12) Kopf (1999); (13) Baldwin et al. (2003); (14) Snoeyenbos et al. (1995) and Baldwin et al. (2004); (15) Bethune et al. (2013); and (16) Dumond et al. (2015). Abbreviations: CLsz, Cora Lake shear zone; EAmT, East Athabasca mylonite triangle; GRsz, Grease River shear zone; LLsz, Legs Lake shear zone; OBSz, Oldman-Bulyea shear zone. Panel modified with permission from Dumond et al. (2010).

The central Snowbird tectonic zone coincides with one of the largest contiguous regions of granulite on Earth—the >20,000-km<sup>2</sup> Athabasca granulite terrane (Figures 3b and 4).

The Athabasca granulite terrane (Figure 3b) consists of medium- to high-pressure granulite and rare eclogite that equilibrated at >0.6 to 1.6 GPa (Figure 4). It occupies the eastern half of the Rae domain exposed north of the 1.7 Ga Athabasca basin at 59–60°N latitude (Figure 4b) (Mahan et al. 2008, Dumond et al. 2010). The terrane likely continues beneath and south of the basin, based on the work of Bickford et al. (1994), Stern et al. (2003), and Card et al. (2007) (Figure 3b). The eastern boundary of the terrane is defined by the Legs Lake thrust-sense shear zone (Mahan et al. 2003, Mahan & Williams 2005, Martel et al. 2008). This >500-km-long shear zone accommodated 1.85 Ga east-vergent uplift with the Athabasca granulite terrane in the hanging wall and low-pressure middle crustal rocks of the Hearne domain in the footwall (Mahan et al. 2003, 2006a,b). The granulite terrane was later offset by ~110 km of right-lateral strike slip across the >400-km-long Grease River shear zone at <1.85–1.8 Ga (Figure 3b) (Mahan & Williams 2005; Dumond et al. 2008, 2013). Similar lower crustal terranes uplifted and exhumed in contractional settings include the Kapuskasing Uplift in the Superior Province of North America (Percival & West 1994) and the Arunta block in the hanging wall of the Redbank thrust in central Australia (Teyssier 1985, Biermeier et al. 2003, Waters-Tormey et al. 2009).

The three most studied portions of the Athabasca granulite terrane (Figure 4a) include polymetamorphic and polydeformed rocks of (a) the East Athabasca mylonite triangle (EAmT) (Hanmer 1994, 1997; Tantato domain of Slimmon & Macdonald 1987); (b) the Snowbird Lake area (Martel et al. 2008); and (c) the Beaverlodge domain (Bethune et al. 2013). The structurally

deepest portions of the terrane coincide with the lithologically heterogeneous EAmt, with high-pressure granulite and crustal eclogite that locally achieved pressures in excess of 1.4–1.6 GPa (**Figure 4b**) (Snoeyenbos et al. 1995; Baldwin et al. 2004, 2007; Dumond et al. 2015). The Snowbird Lake domain is northeast of the EAmt and includes a suite of orthogneisses (metaigneous rocks) and paragneisses (metasedimentary rocks) that experienced pressures of 0.7–1.3 GPa (**Figure 4b**) (Mahan & Williams 2005, Martel et al. 2008, Mahan et al. 2008). The Beaverlodge domain lies west of the EAmt and consists of orthogneisses and paragneisses that locally equilibrated at 0.6–0.8 GPa (**Figure 4b**) (Williams & Jercinovic 2002, Bethune et al. 2013).

One of the major common characteristics of all domains within the Athabasca granulite terrane is ca. 1.9 Ga high-temperature ( $>700^{\circ}\text{C}$ ) and medium- to high-pressure (0.6 to  $>1.0$  GPa) metamorphism and deformation that variably overprinted Neoarchean rocks (**Figure 4b**) (Williams & Hanmer 2006). The 1.94–1.88 Ga period coincided with regional subhorizontal shortening that resulted in the development of several generations of upright, open to tight folds of older fabrics and transposition of folds and gneissic fabrics into steeply dipping to subvertical foliations and northeast-striking mylonitic shear zones (Mahan et al. 2003, 2008; Martel et al. 2008; Ashton et al. 2009; Dumond et al. 2010; Bethune et al. 2013; Regan et al. 2014). These structures are attributed to the 2.0–1.9 Ga Taltson orogeny, the 1.87–1.84 Ga Wopmay orogeny, and the 1.9–1.8 Ga Trans-Hudson orogeny (Dumond et al. 2008, Ashton et al. 2009, Bethune et al. 2013, Regan et al. 2014).

Uplift and exhumation of the Athabasca granulite terrane followed shortly after 1.9 Ga (Flowers et al. 2006a, Mahan et al. 2006a). An early phase of extensional unroofing (from  $\sim 1.1$  to 0.8 GPa) coincident with sinistral transtension is inferred to have occurred before 1.85 Ga (Flowers et al. 2006a, Regan et al. 2014). Dextral transpression occurred at 1.85 Ga coeval with uplift of the terrane from lower crustal ( $>0.8$  GPa) to middle crustal ( $<0.5$  GPa) levels along the Legs Lake and Oldman-Bulyea shear zones (**Figure 4b**) (Mahan et al. 2006a, Dumond et al. 2013). Dextral strike-slip strain at 1.85–1.8 Ga facilitated segmentation of the terrane and other domains along several shear zones throughout the western Churchill Province, including the Grease River and Tyrrell shear zones (**Figures 3b** and **4b**) (MacLachlan et al. 2005a; Dumond et al. 2008, 2013).

## THE ATHABASCA GRANULITE TERRANE FROM THREE PERSPECTIVES

### The East Athabasca Mylonite Triangle

The EAmt is subdivided into three lithotectonic domains: the Chipman domain, the Northwestern domain, and the Upper Deck domain (**Figure 4a**). All three domains contain evidence for high-pressure polymetamorphism and lower crustal polyphase tectonism at ca. 2.61–2.52 and 1.92–1.80 Ga (Williams & Hanmer 2006; Flowers et al. 2008; Mahan et al. 2008, 2011; Williams et al. 2009; Dumond et al. 2010, 2015; Regan et al. 2014, 2017b). The Neoarchean record is dominated by subhorizontal to gently dipping fabrics and recumbent folds associated with lower crustal flow and high-pressure melting (Mahan et al. 2008; Dumond et al. 2010, 2015; Regan et al. 2014, 2017b). The Paleoproterozoic record is characterized by steeply dipping fabrics and shear zones associated with upright tight to isoclinal folds during a second granulite-facies event (Mahan et al. 2008; Dumond et al. 2008, 2010, 2015; Regan et al. 2014). The three domains represent three different deep crustal bulk compositions, and each domain recorded processes that may be characteristic of certain types of deep crust in general.

**Chipman domain.** The Chipman domain is underlain by the  $>3.2$  Ga Chipman tonalite batholith, the ca. 2.59 Ga Fehr granite, the Chipman mafic dike swarm (Macdonald 1980; Flowers

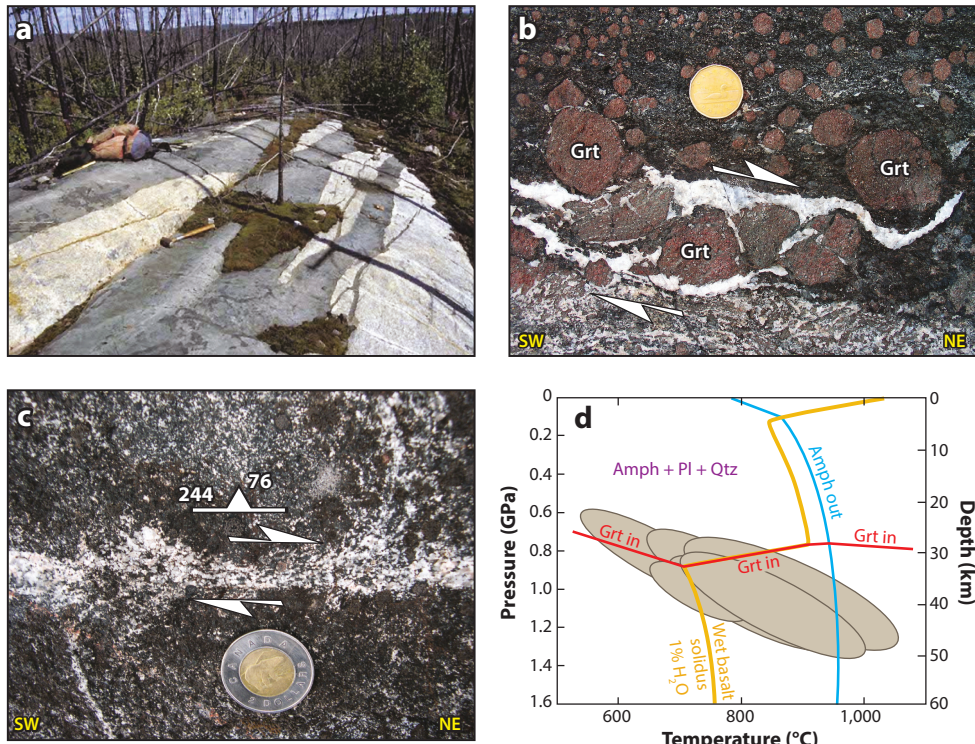


**Figure 5**

(a) Outcrop of Chipman mafic dike. (b) Garnet porphyroblasts with asymmetric tails of tonalite indicating dextral shear sense in a partially molten Chipman dike. (c) Dextral shear band defined by tonalite in a Chipman mafic dike. (d) Petrogenetic grid depicting the garnet in reaction and the wet basalt solidus applicable for the Chipman mafic dikes, after Vielzeuf & Schmidt (2001). The pressure–temperature ( $P$ – $T$ ) 1 $\sigma$  ellipses represent data from Chipman dikes compiled by Mahan & Williams (2005). Abbreviations: Amph, amphibole; Grt, garnet; Pl, plagioclase; Qtz, quartz.

et al. 2006b), and discontinuous meter- to kilometer-scale sheets of garnet-rich felsic and mafic granulite with minor pyroxenite (Figure 4b) (Hanmer 1994; Mahan et al. 2006a, 2008; Flowers et al. 2008). These rock types are virtually identical to and correlated with the so-called Chipman panel described by Martel et al. (2008) in the Snowbird Lake area (Figure 4a; see below). The Chipman dike swarm in the eastern Chipman domain consists of 1–100-m-thick amphibole + plagioclase + garnet + clinopyroxene mafic dikes that were locally partially melted, preserving a record of tonalite melt generation and the production of garnet residue at 1.0–1.2 GPa and 750–850°C (Figure 5) (Williams et al. 1995). Emplacement of at least one component of the dike swarm occurred at 2.1 Ga (Regan et al. 2018), and partial melting of the dikes occurred at 1.896 Ga in association with steep northeast-striking fabric development and dextral shear strain (Figure 5b,c) (Flowers et al. 2006b). Melting of the dike swarm occurred via the fluid-absent amphibole melting reaction  $\text{Amph} + \text{Pl} \rightarrow \text{Grt} + \text{Cpx} + \text{Qtz} + \text{Melt}$  (Figure 5d) (Vielzeuf & Schmidt 2001; mineral abbreviations after Bucher & Frey 2002) and resulted in production of modally abundant garnet with tonalitic leucosome that locally occurs within shear bands and strain shadows adjacent to garnet (Figure 5b,c). Locally, the dike swarm invaded the 2.59 Ga Fehr granite and resulted in extensive crustal melting and hybridization of felsic and mafic magmas (Koteas et al. 2010). The eastern boundary of the Chipman domain coincides with the Legs Lake shear zone.

The western Chipman domain hosts polymetamorphic mafic and felsic granulites that record two episodes of high-pressure, high-temperature metamorphism: at 1.3 GPa, 850–900°C, and at 1.0 GPa, 800–900°C (**Figure 6a**) (Mahan et al. 2006a, 2008). The first episode is related to production of early, subhorizontal to gently dipping gneissic fabrics at ca. 2.55 Ga, and the second, lower-pressure event is interpreted to coincide with steeply dipping and northeast-striking fabric development at ca. 1.9 Ga (**Figure 6b**) (Flowers et al. 2008, Mahan et al. 2008). The western boundary of the Chipman domain is juxtaposed adjacent to the Upper Deck and Northwestern domains of the EAmt along the northeast-striking, steeply northwest-dipping Cora Lake shear zone (Regan et al. 2014). The structure accommodated sinistral transtensional displacement at 1.89–1.87 Ga during the earliest phases of terrane exhumation and an inferred change in the regional stress field coincident with docking of the Lynn Lake and La Ronge arcs along the southern flank of the Churchill Province (Regan et al. 2014). This early phase of exhumation coincided with extensional unroofing and decompression of the Chipman domain (and the EAmt) from ~1.1–1.0 to 0.9–0.8 GPa (Flowers et al. 2006b, Regan et al. 2014).

**Northwestern domain.** The Northwestern domain is predominantly composed of felsic to mafic plutonic bodies bounded on their western margin by the Grease River shear zone (**Figures 4b** and 7). The largest body is the ca. 2.63–2.6 Ga multiphase Mary batholith (Hanmer et al. 1994; Hanmer 1997; Dumond et al. 2010; Regan et al. 2014, 2017b). Granitoids of the Mary batholith were emplaced, metamorphosed, and deformed at 0.9–1.0 GPa and 700–800°C and locally document the progressive transition from charnockite granitoid to garnet granulite gneiss during isobaric cooling and reheating (**Figure 7f**) (Williams et al. 2000, 2014; Dumond et al. 2010; Regan et al. 2014). Bulk rock geochemistry on a suite of rocks from the Mary batholith reveals that it is calc-alkaline in character with enrichment in the large ion lithophile elements and depletions in the high field strength elements, in addition to an enrichment in Pb (Regan et al. 2017b). These data are consistent with the batholith having an arc origin (Regan et al. 2017b). The northern part of the domain consists of the ca. 2.62–2.60 Ga Bohica mafic complex, which represents a suite of gabbroic mafic granulites and anorthosites that are interlayered with the Mary batholith (**Figure 4b**) (Hanmer et al. 1994). The mafic rocks are interpreted to represent the lower portions of a large composite arc batholith (Regan et al. 2017b). Subhorizontal fabric development occurred throughout the Northwestern domain at 2.60–2.55 Ga during penetrative top-to-the-southeast lower crustal flow (**Figure 7d,e**) (Dumond et al. 2010; Regan et al. 2014, 2017b). Meter-scale northeast-striking dextral high-strain zones transpose the early fabrics and appear subparallel to fabrics in the Grease River shear zone. Dates for synkinematic monazite in these zones constrain dextral transpressive strain to 1.92–1.90 Ga (Dumond et al. 2008, 2010).

**Upper Deck domain.** The Upper Deck domain structurally overlies the Northwestern domain along the normal-sense shallowly southwest-dipping Godfrey Bay detachment zone (**Figure 8**) (Hanmer et al. 1995, Dumond et al. 2015). The western boundary of the Upper Deck coincides with the dextral, transpressive Algold Bay shear zone, which records evidence for dextral strain at ca. 1.9 Ga (**Figure 8**) (Dumond et al. 2015). The Upper Deck consists of felsic and mafic granulite gneisses with discontinuous lenses of minor eclogite that record pressures in excess of 1.4–1.6 GPa prior to their juxtaposition with the rest of the EAmt (**Figure 8**) (Snoeyenbos et al. 1995; Baldwin et al. 2003, 2004, 2007; Dumond et al. 2015). Mafic granulite gneisses hosted by the felsic granulites record temperatures of 890–960°C and pressures ranging from 1.3 to 1.9 GPa with two populations of U-Pb isotope dilution–thermal ionization mass spectrometer (ID-TIMS) zircon dates at 2.55–2.52 and 1.9 Ga (Baldwin et al. 2003). Dumond et al. (2015) identified the protolith to the felsic granulite “white gneisses” in the southwestern portion of the domain (**Figure 8**) and applied

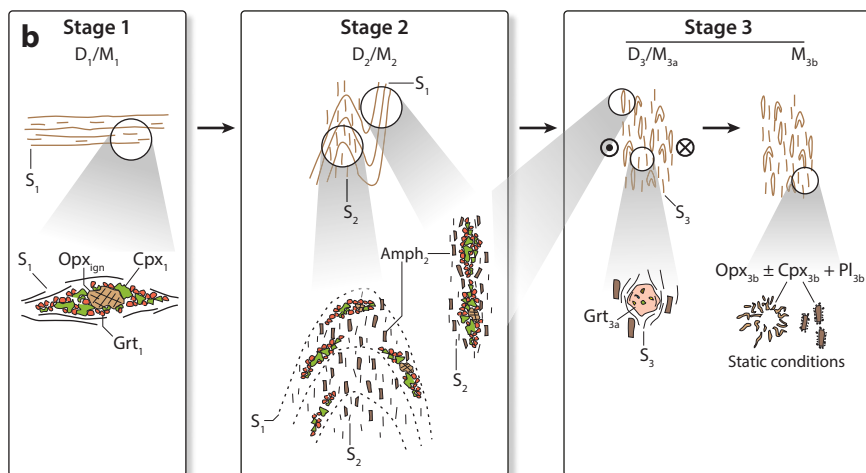
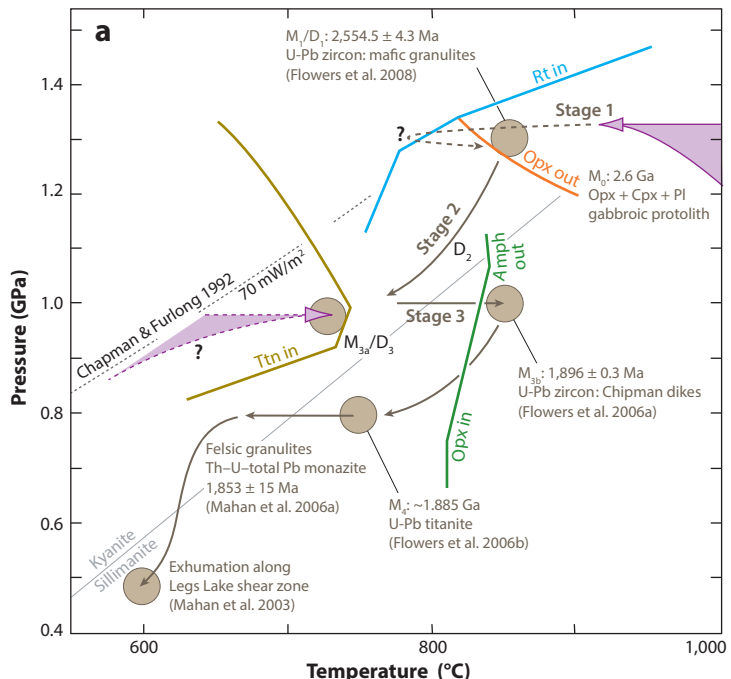


**Figure 6**

(a) Pressure–temperature–time ( $P$ – $T$ – $t$ ) path for high-pressure mafic granulites in the western Chipman domain. (b) Sketch of fabric evolution in mafic granulites. Stage 1 and Stage 3 correspond to the  $P$ – $T$  estimates for Neoarchean and Paleoproterozoic deformation. Abbreviations: Amph, amphibole; Cpx, clinopyroxene; Grt, garnet; Ttn, titanite; Opx, orthopyroxene; Pl, plagioclase; Rt, rutile. Panels *a* and *b* modified from Mahan et al. (2008) with permission.

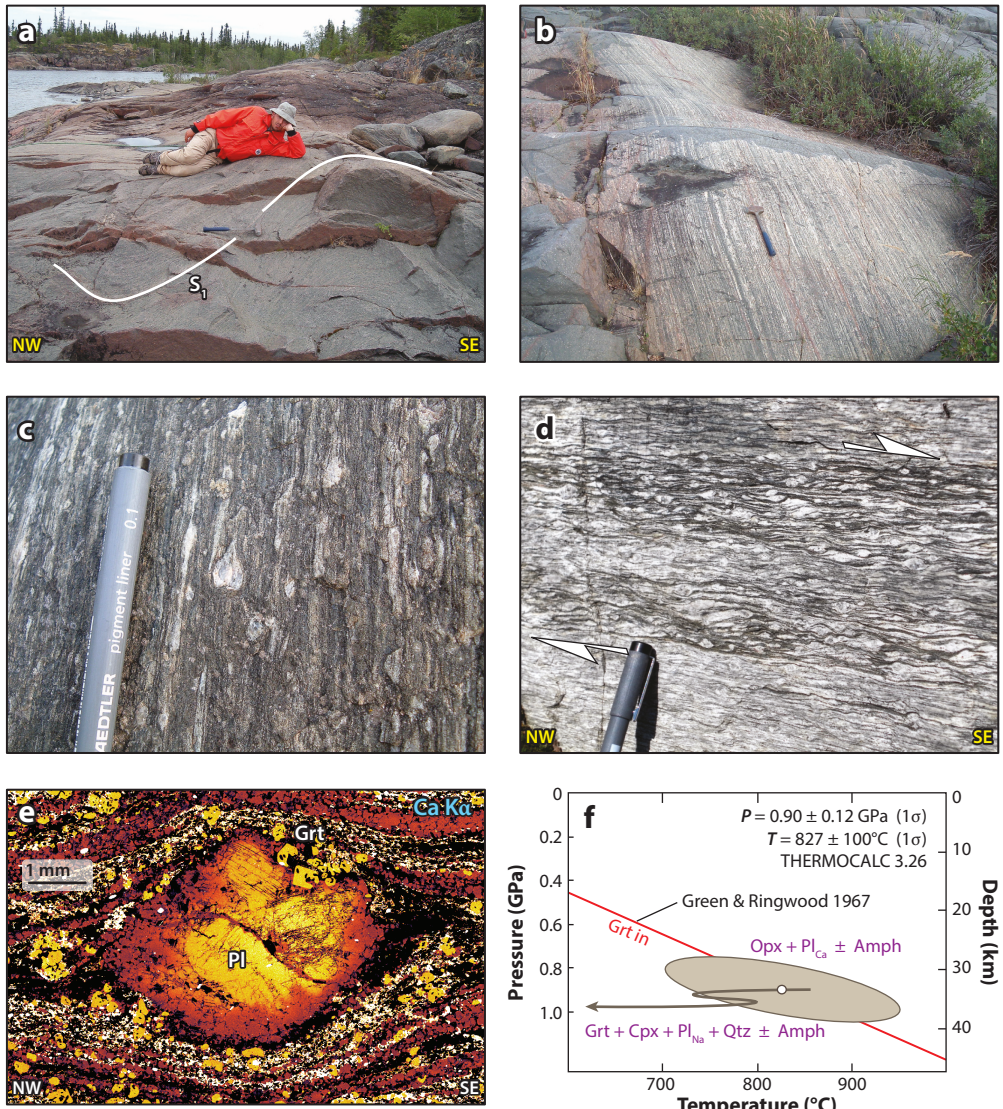


**Figure 7**

Field relationships from the Northwestern domain. (a) Late, upright open folds of originally subhorizontal S<sub>1</sub> gneissic layering. (b) Undulating S<sub>1</sub> foliation surface with penetrative striping lineation developed in thin granite sheet. Note highly noncylindrical nature of late folds due to subtle development of dome-and-basin fold interference pattern. (c) S<sub>1</sub> surface with penetrative lineation development. (d) Top-to-the-southeast sense of shear depicted by C-S fabric developed in granite with subhorizontal fabric. (e) Calcium K $\alpha$  X-ray map illustrating synkinematic garnet that grew at the expense of calcic plagioclase during subhorizontal shear. (f) Pressure-temperature (P-T) conditions of subhorizontal lower crustal flow in the Northwestern domain. Abbreviations: Amph, amphibole; Cpx, clinopyroxene; Grt, garnet; Opx, orthopyroxene; Pl, plagioclase; Qtz, quartz. Panels a–c, e, and f modified from Dumond et al. (2010) with permission. Panel d modified from Regan et al. (2017b) with permission.

## Upper Deck, Athabasca granulite terrane

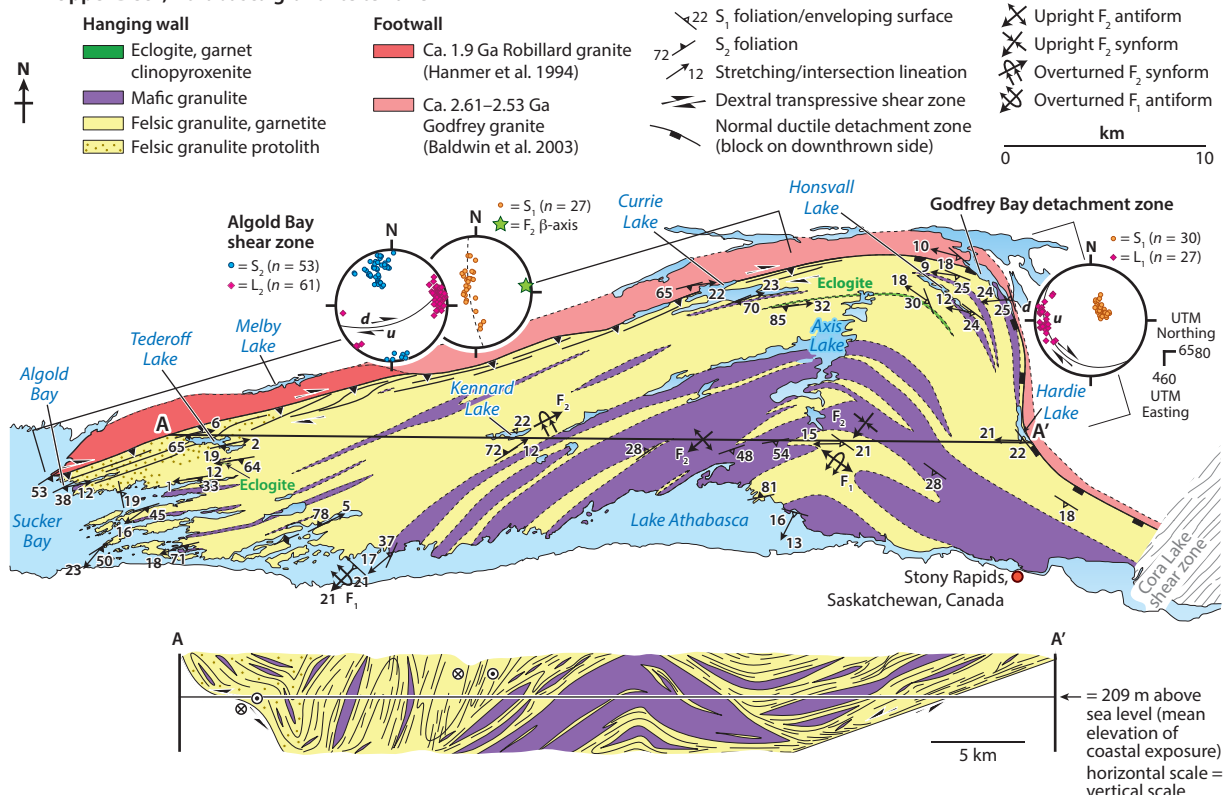


**Figure 8**

Map and cross section of the Upper Deck domain with stereonets for the bounding shear zones. Figure modified from Dumond et al. (2015) with permission.

phase equilibria modeling to the protolith bulk composition. Field relationships demonstrate that partial melting of the protolith was driven by emplacement of the basaltic precursor to the mafic granulites and eclogite, which have primitive mid-ocean ridge basalt (MORB)-like bulk compositions (Figures 9b) (Dumond et al. 2017). Thermodynamic modeling in the NCKFMASHTO ( $\text{Na}_2\text{O}-\text{CaO}-\text{K}_2\text{O}-\text{FeO}-\text{MgO}-\text{Al}_2\text{O}_3-\text{SiO}_2-\text{H}_2\text{O}-\text{TiO}_2-\text{Fe}_2\text{O}_3$ ) system is consistent with the felsic garnet-rich rocks representing the residual products of ultrahigh-temperature melting of the biotite-bearing paragneiss protolith as a response to intraplating of mafic magma in lower continental crust at  $T > 950^\circ\text{C}$  (Dumond et al. 2015). Grossular zoning in the felsic granulite with low-Ca garnet cores that smoothly transition into high-Ca annuli is interpreted to reflect the effects of prograde loading from  $P < 0.8 \text{ GPa}$  to  $P > 1.4 \text{ GPa}$  (Figure 10) (Dumond et al. 2015). Y-depleted monazite dates of 2.61–2.52 Ga constrain the timing of high-pressure partial melting, garnet growth, and crustal thickening (Baldwin et al. 2006; Dumond et al. 2015, 2017).

High-temperature eclogite-facies metamorphism in the Upper Deck was originally interpreted as Neoarchean in age (Snoeyenbos et al. 1995). Baldwin et al. (2004) obtained a zircon U-Pb ID-TIMS date of 1.904 Ga, which was reinforced by ca. 1.9 Ga in situ sensitive high-resolution ion microprobe (SHRIMP) dates on zircon included in jadeite-poor clinopyroxene in a single thin section. Single zircon grains from the same eclogite sample, however, produced a

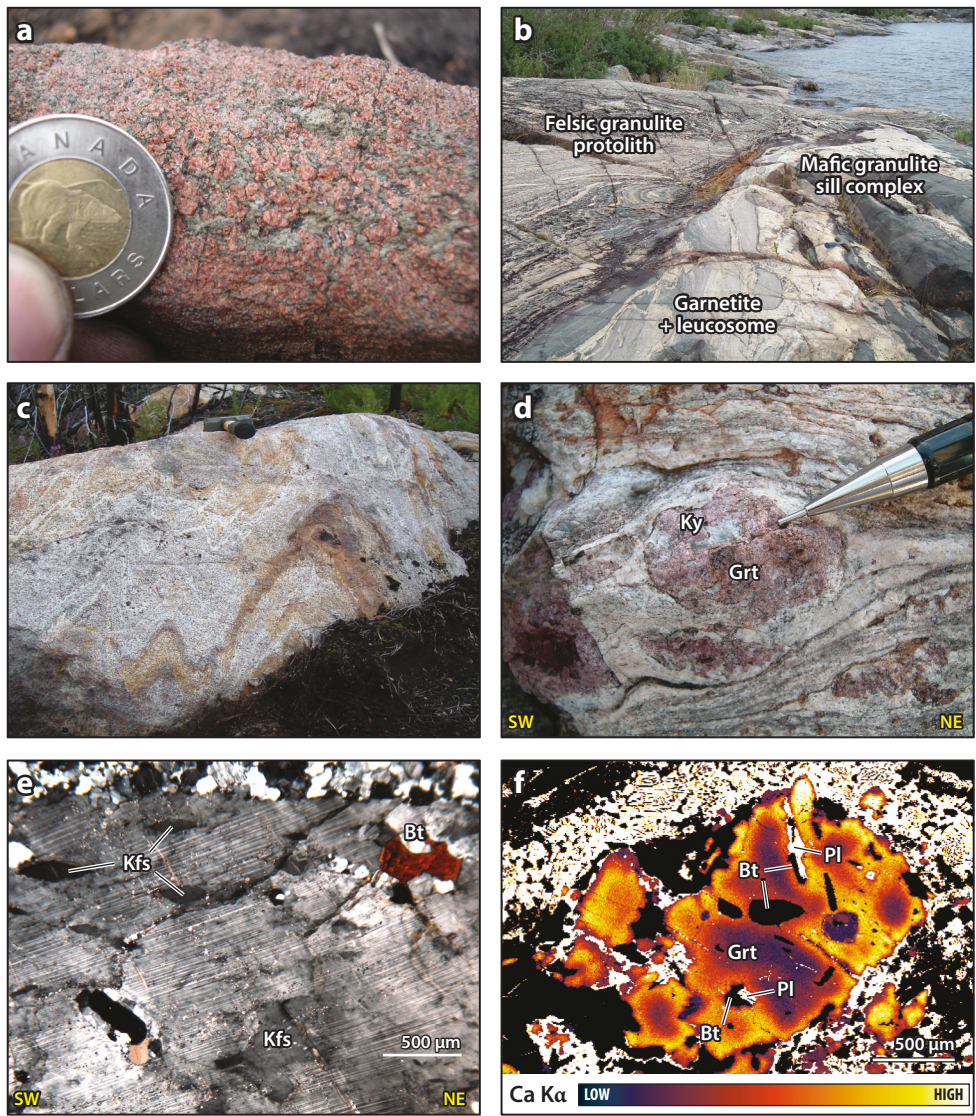


**Figure 9**

Upper Deck field and microstructural relationships. (a) Outcrop of Upper Deck eclogite. (b) Outcrop of mafic granulite sill complex in contact with felsic granulite protolith. Note zone of partial melting indicated by leucosomes and residual garnetite pods. (c) Outcrop of Grt + Ky + Sil felsic granulite ribbon mylonite. Note the early northwest-striking S<sub>1</sub> fabric defined by leucosomes plus layers of garnetite with a gently dipping enveloping surface similar in orientation to outcrop in panel c. (d) Close-up of outcrop of kyanite-bearing felsic granulite. Note inclusion of kyanite in garnet. (e) Cross-polarized photomicrograph of ternary feldspar with inclusion of Ti-rich biotite in felsic granulite. (f) Calcium K $\alpha$  X-ray map illustrating grossular-rich annulus in garnet with inclusions of Bt + Pl, documenting the fluid absent biotite melting reaction in this high-pressure felsic granulite: Bt + Pl + Qtz  $\rightarrow$  Grt + Kfs + Melt. Abbreviations: Bt, biotite; Grt, garnet; Kfs, K-feldspar; Ky, kyanite; Pl, plagioclase; Qtz, quartz; Sil, sillimanite. Panels b and c modified from Dumond et al. (2015) with permission.

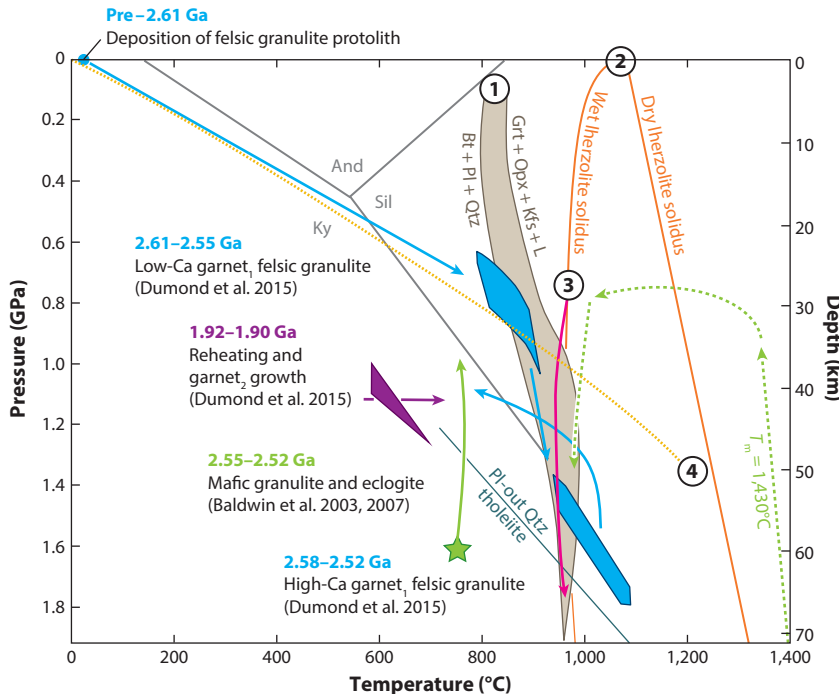


**Figure 10**

Pressure–temperature–time ( $P$ – $T$ – $t$ ) paths for Upper Deck granulites and the eclogite. The blue and purple felsic granulite paths are from Dumond et al. (2015). The solid green mafic granulite and eclogite path is from Baldwin et al. (2003, 2007). The dashed green path is the inferred path for the mafic granulite and eclogite protoliths with mid-ocean ridge basalt generated by decompression melting of fertile lherzolite. A 1,430°C mantle adiabat ( $T_m$ ) is shown for reference (Green et al. 2014). (1) Stability field for fluid-absent biotite melting of metagraywacke (Vielzeuf & Montel 1994). (2) Solidi for fertile lherzolite (Green et al. 2014). (3) Model  $P$ – $T$  path HH100 of Thompson et al. (2001). (4) Hot backarc geotherm modeled for 35-km-thick crust and 50-km-thick lithosphere by Currie & Hyndman (2006). Abbreviations: And, andalusite; Bt, biotite; Grt, garnet; Kfs, K-feldspar; Ky, kyanite; L, liquid; Opx, orthopyroxene; Pl, plagioclase; Qtz, quartz; Sil, sillimanite. Figure modified from Dumond et al. (2017) with permission.

high-precision ID-TIMS U–Pb discordia line with intercepts at 2.54 Ga and 1.91 Ga (Baldwin et al. 2004). In an effort to resolve the timing of metamorphism, Dumond et al. (2017) collected a sample of felsic granulite adjacent to the folded contact of the eclogite layer to obtain in situ Th–U–total Pb monazite dates via electron probe microanalyzer. Three analyses of Y-depleted low-Th monazite inclusions that are interpreted to have grown in equilibrium with high-pressure high-grossular garnet in the felsic granulite–eclogite contact zone yielded a weighted mean date of  $2,529 \pm 34$  Ma ( $2\sigma$ , mean square weighted deviate = 0.11; Dumond et al. 2017), providing a maximum constraint on the timing of garnet growth and high-pressure metamorphism. The occurrence of Neoarchean high-pressure garnet in the eclogite host rock precludes a 1.90 Ga age for eclogite metamorphism and is more consistent with the older concordant U–Pb date of 2.54 Ga obtained for zircon via ID-TIMS by Baldwin et al. (2004). Ca. 1.9 Ga monazite domains in felsic granulite throughout the Upper Deck are inferred to record dissolution–reprecipitation during steep, northeast-striking dextral strain and growth of a second generation of garnet in the felsic granulites that was synchronous with movement along the Algold Bay and Grease River shear zones (Dumond et al. 2015). These data suggest that ca. 1.9 Ga zircon dates in the mafic

granulites and eclogite obtained by Baldwin et al. (2003, 2004) may instead reflect Paleoproterozoic recrystallization of Archean high-pressure assemblages.

## The Snowbird Lake Area

The Snowbird Lake area is northeast of the EAmt and located in the Northwest Territories, Canada (**Figure 4**). The area is subdivided into two lithotectonic domains (**Figure 4a**): the Chipman panel, which is correlative with the Chipman domain of the EAmt (Mahan & Williams 2005, Martel et al. 2008), and the Snowbird Lake domain (Rae Province of Martel et al. 2008). The Snowbird Lake area is offset from the EAmt by 110 km of dextral strike-slip displacement along the Grease River shear zone (**Figure 4**) (Mahan & Williams 2005).

**Chipman panel.** The Chipman panel is underlain by the  $>3.3$  Ga Chipman tonalite batholith and a mafic dike swarm (Martel et al. 2008). The east side of the domain is defined by the northern extension of the Legs Lake shear zone. The west side of the domain is marked by the Striding Athabasca mylonite zone, which has been correlated with the Cora Lake shear zone (**Figure 4**) (Martel et al. 2008). Isolated lenses of mafic and felsic granulite and anorthosite occur throughout the domain. Other rock types occurring as discontinuous layers within the Chipman batholith include mafic granulite, orthopyroxenite, and clinopyroxenite (Martel et al. 2008). Thermobarometry applied to the mafic granulite layers revealed  $P$ - $T$  conditions of 1.35 GPa and 800°C that were inferred to be Neoarchean in age by Mahan et al. (2008). Metagabbro mafic dikes in the Chipman panel occur up to 30 m in width, some varieties contain garnet + tonalitic leucosome, and  $P$ - $T$  conditions for metamorphism of the dikes have been estimated at 1.12 GPa and 795°C (Martel et al. 2008). The dike swarm is inferred to be correlative with the Chipman dike swarm in the EAmt (Mahan & Williams 2005).

Structural analysis of rocks in the Chipman panel reveals early  $S_1$  gneissic fabrics and folds with gently dipping enveloping surfaces that are cut by steeply dipping and northeast-striking  $S_2$  mylonitic fabrics (Mahan & Williams 2005, Martel et al. 2008) that appear similar to structures observed in the Chipman domain in the EAmt (Mahan et al. 2008). The timing of  $S_1$  fabrics is unconstrained, but observation of  $S_2$  fabrics in the Chipman dikes implies a Paleoproterozoic age for  $D_2$  structures (Mahan & Williams 2005, Martel et al. 2008).

**Snowbird Lake domain.** The Snowbird Lake domain (Rae Province of Martel et al. 2008) occurs west of the Chipman panel, adjacent to the Striding Athabasca mylonite zone (Hanmer 1997, Martel et al. 2008). The zone has been correlated with the sinistral Cora Lake shear zone of Regan et al. (2014) in the EAmt, although both dextral and sinistral kinematics have been observed along Snowbird Lake (Martel et al. 2008). The northern part of the Snowbird Lake domain coincides with three metaplutonic orthogneisses: (*a*) the 2.74 Ga Zebra tonalite, with U-Pb zircon evidence for 2.6 Ga metamorphism; (*b*) the 2.66 Ga Camp granodiorite, with U-Pb zircon metamorphic rims at 1.91 Ga; and (*c*) a 2.67 Ga megacrystic granite with 2.61–2.60 Ga titanite (Martel et al. 2008). All three suites are intrusive into a metasedimentary package that includes garnet-bearing paragneisses with leucosome layers indicative of partial melting, in addition to amphibolite, banded iron formation, mafic metavolcanic rocks, and mafic granulite gneiss (Martel et al. 2008). Peak metamorphic conditions of 0.9–1.0 GPa and 800–900°C have been obtained for granulites west of the northern Snowbird Lake domain in the Wholdaia Lake region by Krikorian (2002) (**Figure 4b**).

The southern part of the Snowbird Lake domain includes two rock suites that consist of a metasedimentary package underlain by the 2.55 Ga Rambo granodiorite, which has U-Pb

zircon evidence for 1.92 Ga metamorphism (Martel et al. 2008). Thermobarometry applied to the paragneisses yields  $P$ – $T$  conditions of 0.52–0.76 GPa and 750–840°C, coincident with the rocks experiencing a clockwise  $P$ – $T$ – $t$  path (Martel et al. 2008). The metasedimentary unit consists of interlayered Grt + Sil felsic granulites (metapsammites and metapelites) and minor layers of quartzite and calc-silicate (Martel et al. 2008). Detrital zircon geochronology via SHRIMP was applied to the metapsammite rocks of the southern Snowbird Lake domain, and dates span the range of 2.73–2.06 Ga for detrital zircon cores with metamorphic zircon rims that yield an age of 1.91 Ga, implying that deposition of the sedimentary protolith on top of the exhumed Rambo granodiorite occurred after 2.06 Ga and prior to 1.92–1.91 Ga burial and granulite-facies metamorphism (Martel et al. 2008). These data appear most consistent with the contact between the metasedimentary package and the Rambo granodiorite representing a folded unconformity.

Structural relationships in the southern Snowbird Lake domain indicate two major episodes of deformation. The metasedimentary package and the Rambo granodiorite both contain two generations of folds that define a type 2 mushroom-crescent fold interference pattern. Fabrics related to  $D_1$  include compositional and migmatitic layering in the paragneisses and the granodiorite that are locally folded into northwest-trending isoclinal folds with shallowly to moderately southwest-dipping axial planar surfaces (Martel et al. 2008). Structures related to  $D_2$  include northeast-trending folds with subvertical northeast-striking foliations and axial planes (Martel et al. 2008). Both generations of folds may be interpreted as 1.92–1.91 Ga in age and related to the Taltson orogeny (Martel et al. 2008). Few constraints on the timing and occurrence of Archean deformation were obtained by Martel et al. (2008), and more work is needed to constrain the Neoarchean record in the Snowbird Lake area.

## The Beaverlodge Domain

The Beaverlodge domain is juxtaposed against the EAmt along the >400-km-long and 5–7-km-thick 1.92–1.80 Ga and younger dextral Grease River shear zone (Figures 4 and 11) (Slimmon 1989; Dumond et al. 2008, 2013). The domain consists of polydeformed metasedimentary and metaplutonic gneisses (Figure 11) (Bethune et al. 2013). Two structural levels have been identified separated by what is interpreted as a folded unconformity with rocks below consisting of

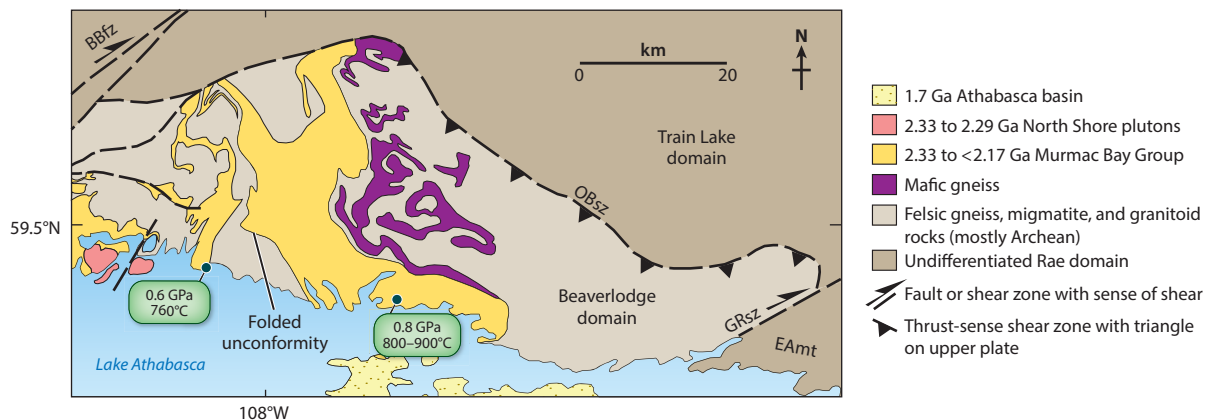


**Figure 11**

Geologic map of the Beaverlodge domain. Abbreviations: BBfz, Black Bay fault zone; EAmt, East Athabasca mylonite triangle; GRsz, Grease River shear zone; OBsz, Oldman-Bulyea shear zone. Figure modified from Bethune et al. (2013) with permission.

2.6–3.1 Ga orthogneisses and paragneisses that are unconformably overlain by supracrustal rocks of the 2.33 to <2.17 Ga Murmac Bay Group (**Figure 11**) (Ashton et al. 2013, Bethune et al. 2013, Shiels et al. 2016). The domain is intruded by the North Shore plutons, a suite of 2.33–2.29 Ga granites (Hartlaub et al. 2007).

Rocks of the deepest structural level of the Beaverlodge domain consist of high-grade Archean orthogneisses and paragneisses that variably record the effects of Neoarchean (ca. 2.57 Ga) and Paleoproterozoic (ca. 2.5–2.3 Ga and 1.94–1.90 Ga) tectonism. Three suites of orthogneisses are recognized at this structural level: 3.06–2.99 Ga granites, 2.68–2.60 Ga granites, and 2.33–2.29 Ga granites (Hartlaub et al. 2005, 2007; Bethune et al. 2013). These orthogneisses occur in association with migmatitic paragneisses that contain U–Pb zircon and monazite evidence for both 2.57 Ga and 2.5–2.3 Ga metamorphism (Bethune et al. 2013). Fabrics associated with the Archean and 2.5–2.3 Ga “Arrowsmith” events are not well constrained (Bethune et al. 2013). More work is needed to constrain the Neoarchean and Arrowsmith records in the Beaverlodge domain, especially with regards to linking zircon and monazite dates to specific fabrics and structures in the deepest structural levels. Ca. 1.94–1.90 Ga structures are present throughout and are associated with east-southeast-striking transposition foliations and tight to isoclinal folds that were refolded into northwest-trending open folds (Bethune et al. 2013). These structures were overprinted by northeast-striking fabrics, folds, and dextral mylonitic shear zones dated at ca. 1.90 Ga and associated with dextral transpression along the Grease River shear zone (Dumond et al. 2008, 2010, 2015; Bethune et al. 2013).

The 2.33 to <2.17 Ga Murmac Bay Group defines the upper structural level of the Beaverlodge domain. The most recent detrital zircon work revealed that the upper Murmac Bay Group was deposited between 2.00 and 1.94 Ga (Shiels et al. 2016). This ~1-km-thick sedimentary succession is variably affected by greenschist- to granulite-grade metamorphism (Williams & Jercinovic 2002, Bethune et al. 2013). Where the rocks are least overprinted, the succession consists of basal conglomerate and quartzite to psammite that is locally intercalated with dolostone, iron formation, and mafic volcanic flows, all of which are overlain by psammopelite to pelite gneisses (Ashton et al. 2013). Exposures of this upper structural level are devoid of Archean rocks and do not record the effects of the 2.5–2.3 Ga “Arrowsmith” event (Ashton et al. 2013, Bethune et al. 2013). Following <2.17 Ga deposition of the upper Murmac Bay Group, peak metamorphic conditions were attained during 1.94–1.90 Ga tectonism and reached 0.6–0.8 GPa and 760–850°C, coincident with a clockwise  $P$ – $T$ – $t$  path (Williams & Jercinovic 2002, Bethune et al. 2013). Bethune et al. (2013) interpreted these conditions to represent the effects of thrusting during the Taltson orogeny along the southern margin of the Rae domain. Loading of the crust during the Taltson orogeny was followed by decompression and breakdown of garnet to cordierite at ca. 1.91–1.90 Ga (Bethune et al. 2013).

## TECTONIC IMPLICATIONS FOR THE WESTERN CANADIAN SHIELD FROM THE ATHABASCA GRANULITE TERRANE

Research in the Athabasca granulite terrane has revealed a noteworthy dichotomy: Whereas the Archean record of tectonism is well preserved in the EAmt (Baldwin et al. 2003, 2006; Flowers et al. 2008; Mahan et al. 2008; Dumond et al. 2010, 2015, 2017; Regan et al. 2017a,b), the Snowbird Lake and Beaverlodge domains have well-preserved Paleoproterozoic records and much more cryptic Archean records (Martel et al. 2008, Bethune et al. 2013). These two perspectives are not mutually exclusive, and the principal differences between these lithotectonic domains may, in part, be due to the duration that each resided in the middle to lower crust prior to uplift and exhumation to the surface. Folded unconformities exposed in the Beaverlodge and Snowbird Lake domains

document the record of post-Neoarchean uplift and exhumation of middle to lower continental crust that was subsequently reburied in the Paleoproterozoic at 1.94–1.90 Ga (Martel et al. 2008, Bethune et al. 2013). No such unconformity has been identified in the EAmt, and crust exposed there has been hypothesized to record long-term (>650 Myr) lower crustal residence following Neoarchean tectonism and subsequent to Paleoproterozoic reheating and reactivation (Williams & Hanmer 2006, Flowers et al. 2008, Mahan et al. 2008). Whereas rocks in the Snowbird Lake and Beaverlodge domains contain cordierite and evidence for high-temperature decompression in the Paleoproterozoic (Martel et al. 2008, Bethune et al. 2013), rocks in the EAmt are devoid of cordierite and record isobaric cooling paths following decompression in the Neoarchean to lower crustal levels (Figures 6a and 10) (Williams et al. 2000, Mahan et al. 2008, Dumond et al. 2015). Subsequent Paleoproterozoic decompression and uplift to the surface affected the EAmt and other domains between 1.9 and 1.7 Ga (Figure 6a) (Baldwin et al. 2003, 2004, 2007, 2015; Mahan et al. 2006a; Flowers et al. 2006b; Bethune et al. 2013). Below we summarize the implications for Archean and Paleoproterozoic tectonism that have been gleaned from these lithotectonic domains and the constraints they provide on the evolution of the western Canadian Shield between 2.6 and 1.7 Ga, in addition to implications for the character and behavior of lower continental crust in general.

## The Archean Record of the Athabasca Granulite Terrane

The oldest crust present in the Athabasca granulite terrane is represented by the >3.2 Ga Chipman tonalite batholith in the EAmt and Snowbird Lake area (Hanmer et al. 1994, Martel et al. 2008). Mesoarchean granites are also present in the Beaverlodge domain, occurring as the 3.1–3.0 Ga Lodge Bay and Cornwall Bay granites along with evidence for older crust preserved as >3.6 Ga zircon xenocrysts in younger granites (Hartlaub et al. 2005). These basement rocks were intruded by voluminous Neoarchean (2.68–2.55 Ga) granites (Hanmer et al. 1994, Hartlaub et al. 2005, Martel et al. 2008, Bethune et al. 2013). Work on the ca. 2.63–2.60 Ga Mary batholith in the EAmt is most consistent with this suite of rocks representing a continental arc (Regan et al. 2017b). Arc rocks in the EAmt were subsequently overprinted by penetrative lower crustal flow and subhorizontal fabric development at 2.60–2.55 Ga (Dumond et al. 2015, Regan et al. 2017b). Neoarchean lower crustal flow preserved in the Mary batholith temporally overlaps with  $S_1$  fabric development and high-pressure metamorphism (1.3 GPa and 850–900°C) preserved in mafic granulites of the adjoining Chipman domain (Figure 6a) (Flowers et al. 2008, Mahan et al. 2008). This record of lower crustal flow also coincides with the period of melting and garnet-rich residue production documented in felsic granulite paragneisses of the overlying Upper Deck domain at ca. 2.61–2.52 Ga (Figure 10) (Baldwin et al. 2006, Dumond et al. 2015). Thus, the entire EAmt preserves evidence for a protracted period of lower crustal flow and subhorizontal fabric development, despite variations in lithology and age. Regan et al. (2017b) proposed that the eastern Rae domain at 2.62–2.50 Ga was the locus of a continental arc that transitioned into a collisional tectonic setting. Dumond et al. (2017) inferred that the Upper Deck domain was constructed in a backarc basin setting adjacent to this continental arc that was subsequently closed and thickened coincident with ultrahigh-temperature metamorphism, thus juxtaposing a backarc with a continental arc along the Upper Deck boundary at 2.54 Ga.

Neoarchean (ca. 2.62–2.50 Ga) plutonism, deformation, and/or metamorphism have been identified throughout much of the Churchill Province (Hanmer et al. 1994, 2006; Snoeyenbos et al. 1995; Williams et al. 2000; Sanborn-Barrie et al. 2001; Stern & Berman 2001; MacLachlan et al. 2005b; Baldwin et al. 2006; Mills et al. 2007; Flowers et al. 2008; Mahan et al. 2008; Martel et al. 2008; Dumond et al. 2010, 2015, 2017; Bethune et al. 2013; Regan et al. 2017b).

The Neoarchean record of tectonometamorphism in the Athabasca granulite terrane appears to be coincident with that preserved in the Chesterfield (Northwestern Hearne) domain (**Figure 3b**) (Stern & Berman 2001, MacLachlan et al. 2005b, Davis et al. 2006, Hanmer et al. 2006). Subhorizontal, top-to-the-southeast lower crustal flow documented in the EAmt may correlate with Neoarchean southeast-vergent thrusting observed or inferred along the Tyrell shear zone in the Yathkyed Lake supracrustal belt (MacLachlan et al. 2005b) and along the Big Lake shear zone that floors the Cross Bay plutonic complex further northeast (Hanmer et al. 2006). This correlation implies an 800-km-long region of top-to-the-southeast strain that is subparallel to the Snowbird tectonic zone and may support a Neoarchean collisional origin for at least part of this >2,800-km-long lineament (Jones et al. 2002; Regan et al. 2017a,b). Two models for this event, termed the MacQuoid orogeny, include collision of the Chesterfield domain with the Rae domain (MacLachlan et al. 2005b, Davis et al. 2006, Berman et al. 2007, Pehrsson et al. 2013) and/or collision of the Hearne domain with the Rae domain (Aspler & Chiarenzelli 1996, Jones et al. 2002, Regan et al. 2017b). Hafnium isotopes analyzed in zircon from 2.60 Ga igneous rocks show little variation in  $\epsilon_{\text{Hf}}$  across the central Snowbird tectonic zone, consistent with no major crustal discontinuity at the Rae–Hearne boundary in the southern Churchill Province (Regan et al. 2017a). Ca. 2.60–2.55 Ga magmatism, metamorphism, and deformation occur on both sides of the boundary at the latitude of 59–60°N, supporting the interpretation that the eastern Rae and southern Hearne domains were contiguous by 2.60 Ga (Regan et al. 2017b). These data are consistent with the findings of Cousens et al. (2001), who studied Nd isotopes in 1.83 Ga ultrapotassic rocks across the northern and central Churchill Province and concluded that enriched metasomatized Archean lithospheric mantle exists on both sides of the Snowbird tectonic zone, further supporting the interpretation that the Rae and Hearne domains were contiguous in the Archean. Alternatively, Berman et al. (2007) suggested that only the Chesterfield domain was sutured to the Rae domain in the Neoarchean, leaving the rest of the central and southern Hearne domains to collide with the Rae domain in the Paleoproterozoic during a 1.9 Ga event termed the Snowbird orogeny.

## The Paleoproterozoic Record of the Athabasca Granulite Terrane

Four major orogenic events and at least one episode of rifting are interpreted to have affected the Churchill Province in the vicinity of the Athabasca granulite terrane prior to the 1.74–1.73 Ga deposition of the basal section of the Athabasca basin (Rainbird et al. 2007). These include (a) the 2.5–2.3 Ga Arrowsmith orogeny (Berman et al. 2005, 2013), (b) the ca. 2.1 Ga emplacement of mafic dike swarms during incipient rifting of the Churchill Province (Regan et al. 2018), (c) the 2.0–1.9 Ga Taltson orogeny (McDonough et al. 2000, Martel et al. 2008, Bethune et al. 2013, Card et al. 2014), (d) the 1.88–1.84 Ga Wopmay orogeny (Hildebrand et al. 2010, Regan et al. 2014), and (e) the 1.9–1.8 Ga Trans-Hudson orogeny (Ansdel 2005, Dumond et al. 2008). A case has been made for a separate 1.9 Ga Snowbird event (Berman et al. 2007), but following the work of Bethune et al. (2013), we suggest that it is part of a continuum of deformation related to the end of the Taltson orogeny and the onset of the Trans-Hudson orogeny.

**The 2.5–2.3 Ga Arrowsmith orogeny.** The Arrowsmith orogeny is interpreted as the consequence of collision of either the Slave Province or an unidentified terrane along the western margin of the Rae domain between 2.5 and 2.3 Ga (Berman et al. 2013, Card et al. 2014). The only record of this identified so far in the Athabasca granulite terrane occurs in the Beaverlodge domain, which contains the 2.33–2.28 Ga North Shore plutons. This suite of intrusions has been interpreted as syn- to postcollisional granites that do not appear to have an arc affinity (Hartlaub et al. 2007). Further evidence in the domain was discovered by Bethune et al. (2013), who identified

2.46–2.24 Ga metamorphic zircon overgrowths in the 2.68 Ga Deadman granite. Deformation fabrics related to the Arrowsmith orogeny have not yet been identified in the Athabasca granulite terrane, and more data are needed to constrain the impact of this event.

**Incipient intracontinental rifting and ca. 2.1–1.9 Ga mafic magmatism.** Mafic magmatism parallels the eastern margin of the Athabasca granulite terrane along much of its length and broadly corresponds to the geophysical expression of the Snowbird tectonic zone (Flowers et al. 2006a). The Chipman dike swarm was emplaced into the Mesoarchean Chipman tonalite in both the EAmt and Snowbird Lake regions and is bound on the east by the Legs Lake shear zone (Mahan et al. 2003) and on the west by the Cora Lake shear zone (EAmt; Regan et al. 2014) and the Striding mylonite zone (Snowbird Lake domain; Martel et al. 2008). Constraining a crystallization age has been difficult owing to a mafic composition and granulite-grade metamorphic overprint (1.17 GPa and  $>775^{\circ}\text{C}$ ; Williams et al. 1995). New *in situ* secondary ionization mass spectrometry microzircon geochronology of grains with morphology and composition consistent with an igneous origin yielded a ca.  $2,113 \pm 13$  Ma date (Regan et al. 2018). This result is corroborated by microzircon geochronology of the Kazan dikes from the Angikuni Lake region (Fahrig et al. 1984), which yielded an indistinguishable age. Geochemistry and Nd isotopic analyses from both dike swarms (Flowers et al. 2006a, Regan et al. 2018) indicate an asthenospheric source that underwent substantial contamination from a thick Archean lithospheric root (Flowers et al. 2006a, Regan et al. 2018). The timing and composition correspond well with extensive gabbro sill injections in the neighboring central Hearne domain of the western Churchill Province (Griffin gabbros; Aspler et al. 2002) and, more broadly, with widespread extensional tectonics preserved throughout the western Canadian Shield (Aspler et al. 2002). Magmatism associated with the Chipman and Kazan dike swarms extends for well over 800 km along strike and may help explain the narrow gravity anomaly, which delineates the eastern margin of the Athabasca granulite terrane. Based on synkinematic relationships provided by Williams et al. (1995) and Koteas et al. (2010), it is possible that a second generation of mafic dikes was emplaced at ca. 1.9 Ga. The geographic extent or tectonic setting of a possible second swarm has not yet been determined.

**Paleoproterozoic reactivation during assembly of Nuna supercontinent.** Paleoproterozoic tectonism within the Athabasca granulite terrain extends from 1.93 to 1.80 Ga and involved the development of subvertical to moderately dipping structural fabrics (Mahan et al. 2003, 2008; Flowers et al. 2006b, 2008; Martel et al. 2008; Williams et al. 2009; Dumond et al. 2008, 2010, 2013; Bethune et al. 2013; Regan et al. 2014). Peak metamorphic conditions at 1.9 Ga correspond with upright folding and dextral strike-slip to oblique-slip deformation over a wide region ( $>40$  km wide across strike). Subsequent tectonism was localized into thick ductile shear zones of varying grade and records progressive uplift of the terrane during multistage exhumation and juxtaposition of lithotectonic blocks (Flowers et al. 2006b).

The Cora Lake shear zone juxtaposed Neoarchean plutonic rocks of the Northwestern subdomain adjacent to slightly deeper (higher-pressure) rocks of the Chipman subdomain during sinistral transtension from 1.89 to 1.87 Ga (Regan et al. 2014). This was followed by renewed dextral deformation during contractional uplift along the Legs Lake shear zone, and the episodic activity of several other shear zones in the area, including the Oldman-Bulyea shear zone and Grease River shear zone from 1.85 to 1.80 Ga (Mahan et al. 2003, 2006a,b; Dumond et al. 2008, 2013). This phase of tectonism resulted in the juxtaposition of the Athabasca granulite terrane structurally above lower-grade and lower-pressure rocks of the Hearne domain (Mahan et al. 2003). Uplift was followed by protracted exhumation and lower-amphibolite to greenschist-facies reactivation of the Grease River shear zone at 1.82–1.80 Ga, which accommodated 110 km of right-lateral

offset calculated by using the intersection of the Chipman dike swarm with an isobaric surface (1.17 GPa) as a piercing point (Mahan & Williams 2005). Despite the range in metamorphic conditions and kinematics, all the shear zones contain a similarly oriented stretching lineation, generally plunging shallowly to the southwest or northeast.

The western Churchill Province was host to arc-accretion and collisional processes on both margins from 1.98 to 1.80 Ga (Hoffman 1988). Collision with the Slave Province and Buffalo Head terrane occurred from 1.98 to 1.90 Ga during the Taltson and Thelon orogenies along the western margin of the Churchill Province (**Figure 3**) (Hoffman 1988, Card et al. 2014). Reactivation and further indentation of the Slave craton into the Churchill craton occurred at 1.86 Ga during the Wopmay orogeny on the western margin of the Slave craton (Hanmer et al. 1992, Hildebrand et al. 2010). Accretionary processes along the southern periphery of the Churchill Province involved collision with the Lynn Lake and La Ronge arcs followed by rollback tectonics and culminating with the collision of the Sask and Superior cratons at 1.82 Ga (Chiarenzelli et al. 1998, Corrigan et al. 2009). Based on the summary provided by Regan et al. (2014), widespread tectonism and dextral strike-slip deformation in the Athabasca granulite terrane occurred during the latter phases of Taltson-Thelon orogenesis. Sinistral deformation, within the Cora Lake shear zone, occurred during accretion of the Lynn Lake and La Ronge arcs along the southern margin of the Churchill Province. Renewed indentation of the Slave craton into the Churchill Province corresponds with oblique dextral shearing within the Legs Lake and Grease River shear zones during contractional uplift of the Athabasca granulite terrane, as documented by Mahan et al. (2003) and Dumond et al. (2008, 2013). It is expected that the mechanisms and driving forces for this far-field tectonism will be refined with better understanding of the bounding orogens.

## GENERAL IMPLICATIONS FOR LOWER CONTINENTAL CRUST FROM THE ATHABASCA GRANULITE TERRANE

### Compositional Evolution of Lower Continental Crust

Bulk compositions of rocks from the Athabasca granulite terrane span virtually the entire range of compositions observed in granulites worldwide, with 43–75 wt% SiO<sub>2</sub>, 14–83 molar Mg#, and Eu anomalies of 0.33–3.67 (**Figure 1**; **Supplemental Table 1**). The database in **Supplemental Table 1** consists of 84 samples ranging from mafic granulites and eclogites to felsic granulites, tonalites, and arc-related granitoids. The peraluminous felsic granulites have bulk compositions similar to upper continental crust (**Figure 12**). Felsic granulite protoliths display rare earth element (REE) patterns similar to those of graywackes and shales (**Figure 12c**), consistent with these originally being supracrustal metasedimentary rocks. The arc-related granitoids of the Mary batholith are calc-alkaline in character (**Figure 13a**) and exhibit large ion lithophile element enrichment and depletions in the high field strength elements (**Figure 13b**). The mafic granulites, eclogites, and Chipman mafic dikes exhibit tholeiitic trends on an AFM diagram (**Figure 13a**). Mafic granulites and Chipman dikes have compositions similar to tholeiitic basalts, whereas the eclogites have high-alumina basalt compositions. Mafic granulites, eclogites, and Chipman dikes have bulk compositions that are similar to primitive MORB (**Figure 13c–b**). The eclogite and Chipman dike samples tend to have negatively sloping patterns due to light REE enrichment (**Figure 13c,g**), and many eclogite samples have positive Eu anomalies indicative of plagioclase accumulation (**Figure 13c,d**).

A bulk lower crustal composition was derived using the most studied portion of the Athabasca granulite terrane: the 2,566-km<sup>2</sup> EAmt, which consists of 35.36% arc-related granitoid, 19.81% mafic granulite, 18.66% felsic granulite, 18.43% tonalite, 7.69% Chipman mafic dike, and 0.04%

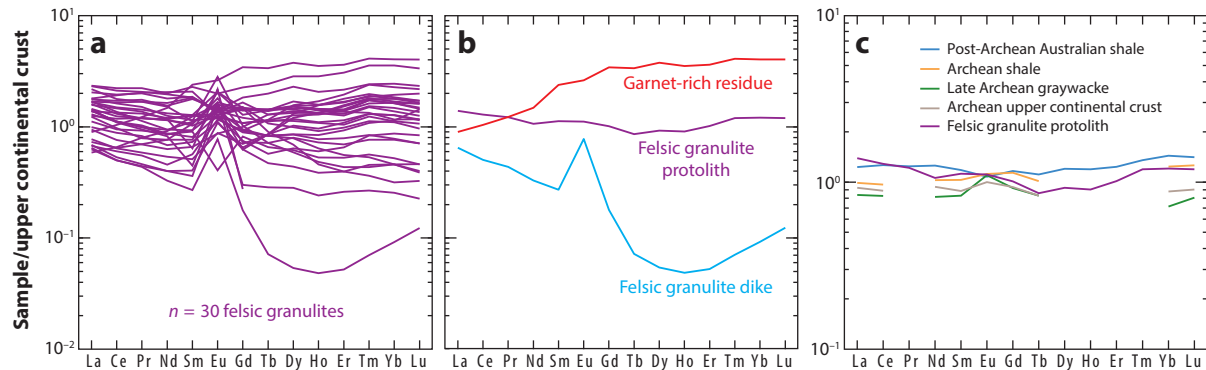


**Figure 12**

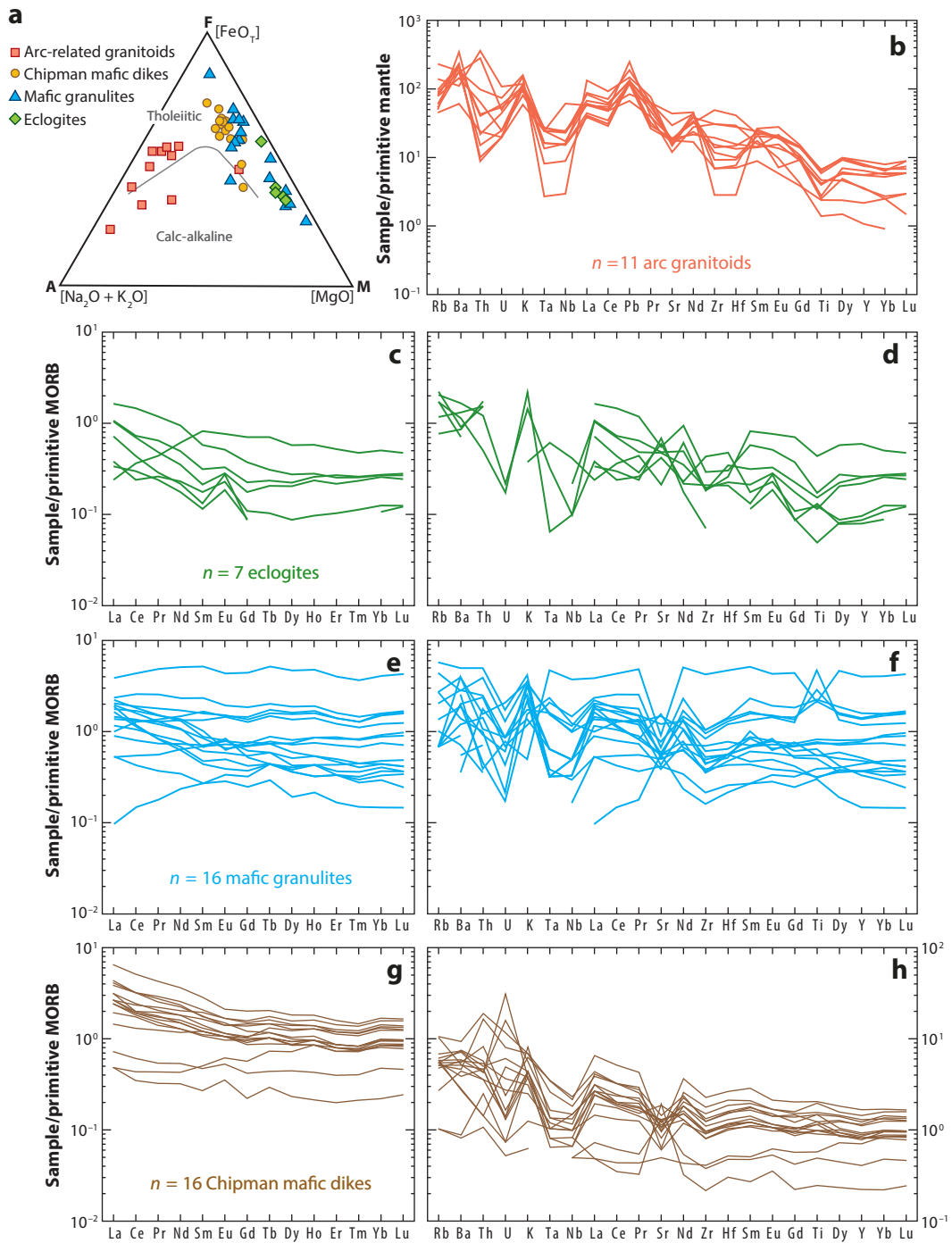
Bulk geochemistry for felsic granulites and protolith. (a) Rare earth element (REE) diagram normalized to the upper continental crust composition from Rudnick & Gao (2003). (b) REE diagram depicting the differences between the felsic granulite protolith, dike, and residual garnetite. (c) REE diagram showing comparison of the felsic granulite protolith with other sedimentary bulk compositions taken from Condie (1993).

eclogite (Figure 4b). This bulk composition (60 wt%  $\text{SiO}_2$ ;  $\text{Mg}\# = 44$ ) plots within the range of lower crustal compositions derived by Hacker et al. (2015) (E in Figure 1). From the perspective of the EAmt, this lower crustal bulk composition evolved with time. The terrane was originally more felsic, containing the Chipman tonalite and felsic granulite paragneisses. These rocks were intruded by the Mary batholith and other arc-related granitoids (involving a range of mafic to felsic compositions). The bulk composition became more mafic as these rocks were intruded by the protoliths to the mafic granulites, e.g., the Bohica mafic complex, the Upper Deck mafic granulite sill complex, and mafic granulite lenses in the Chipman domain. Finally, the EAmt became even more mafic due to emplacement of the Chipman dike swarm prior to the onset of terrane uplift and exhumation post-1.9 Ga.

### Crustal Densification and Implications for Seismic Velocity, Crustal Root Growth, and Foundering

The lower continental crust can undergo significant densification, crustal root development, and/or foundering of deep crust (Fischer 2002, Schulmann et al. 2005, Ducea 2011). Rocks from the EAmt have been used to constrain the effect of densification on the lower crust (Williams et al. 2014), demonstrating that felsic rocks can be significant contributors to increasing lower crustal density and seismic velocity. We mention three examples here, focused on metaluminous orthogneisses and peraluminous felsic granulite paragneisses with associated mafic granulites (Figure 14). Phase equilibria diagrams using these bulk compositions were calculated with Perple\_X 6.7.7 (Connolly 2005) using the updated thermodynamic database of Holland & Powell (1998) augmented with adiabatic bulk and shear moduli data from Connolly & Kerrick (2002) and Hacker & Abers (2004), including a piecewise linear fit to the properties of quartz from Ohno et al. (2006) to more realistically model the  $\alpha$ – $\beta$  quartz transition.

Felsic orthogneisses represent a volumetrically significant component of the EAmt (35.36%) and are noteworthy for the occurrence of the synkinematic reaction  $\text{Opx} + \text{Ca-rich Pl} \rightarrow \text{Grt} + \text{Cpx} + \text{Na-rich Pl} + \text{Qtz}$  (Williams et al. 2000, 2014). This reaction represents the transition from medium-pressure to high-pressure granulite derived by Green & Ringwood (1967). The



(Caption appears on following page)

**Figure 13** (Figure appears on preceding page)

(a) AFM diagram for mafic rocks and arc-related granitoids in the Athabasca granulite terrane. (b) Spider diagram for arc-related granitoids of the East Athabasca mylonite triangle (EAmt) normalized to the primitive mantle composition from McDonough & Sun (1995). (c,d) Eclogite bulk compositions of the EAmt normalized to the primitive mid-ocean ridge basalt (MORB) composition from Kelemen et al. (2003). (e,f) Mafic granulite bulk compositions of the EAmt normalized to the primitive MORB composition from Kelemen et al. (2003). (g,b) Chipman mafic dike bulk compositions of the EAmt normalized to the primitive MORB composition from Kelemen et al. (2003).

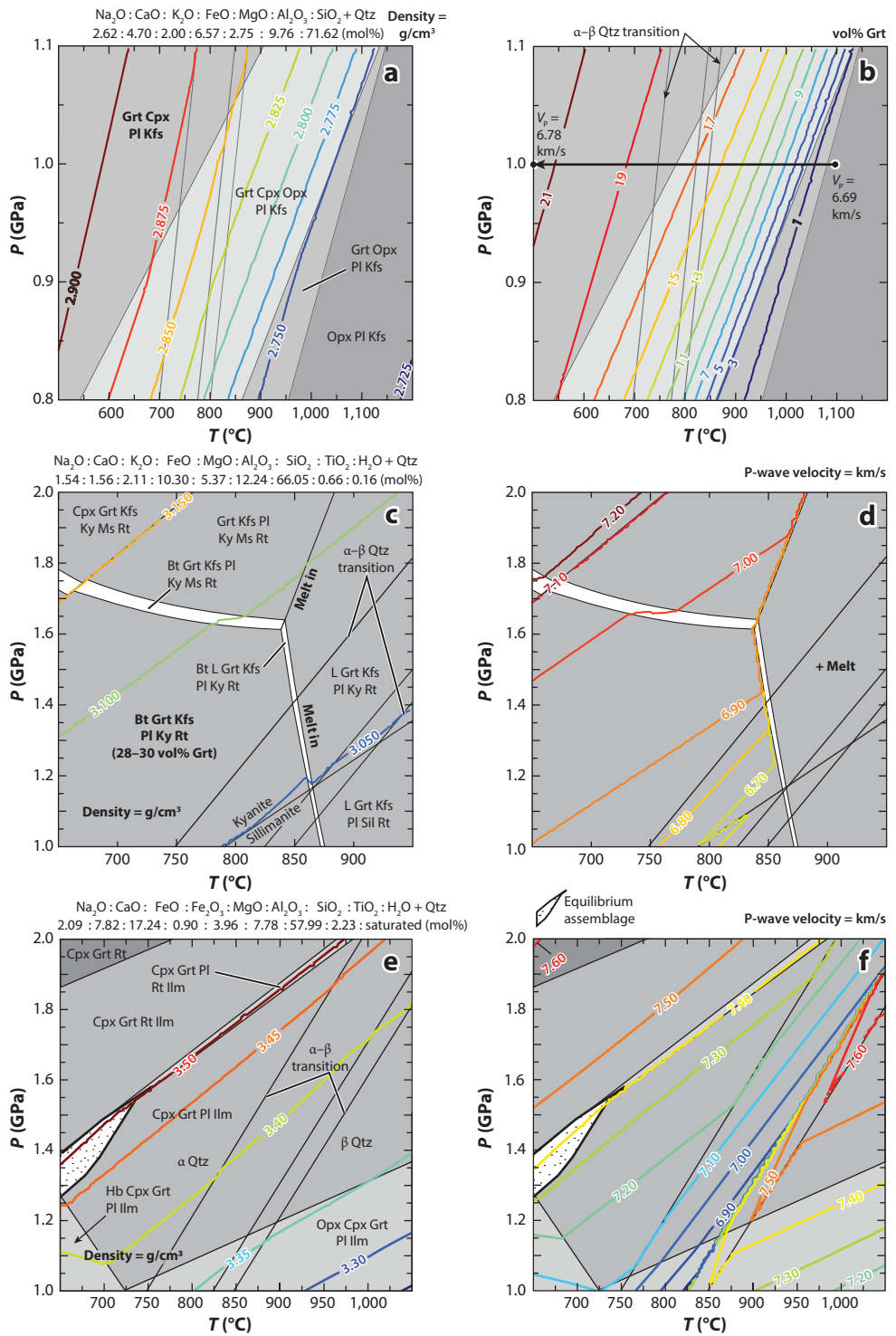
reaction is crossed during isobaric cooling  $\pm$  reheating at lower crustal levels, e.g., 1.0 GPa (Figure 14a,b). Rocks along this cooling path evolve with increased volumes of Grt + Cpx and bulk densities approaching 2.9–3.0 g/cm<sup>3</sup> (Figure 14a). Felsic orthogneisses that equilibrate at 1.0 GPa have P-wave velocities approaching 6.8 km/s (Figure 14b). Felsic granulite paragneisses represent a second volumetrically abundant (18.66%) bulk composition that can have appreciable amounts of garnet. The paragneisses experienced significant melting and garnet growth due to the reaction  $\text{Bt} + \text{Pl} + \text{Qtz} \rightarrow \text{Grt} + \text{Kfs} + \text{Melt}$  (Dumond et al. 2015). Phase equilibria diagrams for garnet-rich residual bulk compositions produce significant amounts of garnet (28–30 vol%), high densities (>3.1 g/cm<sup>3</sup>), and P-wave velocities of >7.00 km/s (e.g., equilibrating at  $P > 1.4$ –1.6 GPa and  $T = 650$ –700°C; Figures 14c,d). These results suggest that high-velocity lower continental crust can have a significant component of felsic rocks, as inferred by Hacker et al. (2011, 2014, 2015; see also Massonne et al. 2007).

Mafic rocks are also an important component of EAmt lower crust (27.54% as determined above, including mafic granulites, mafic dikes, and eclogite). This value falls within the estimates of Hacker et al. (2015), who concluded that 20–30% of lower crust beneath shields should consist of mafic rocks. Mafic granulites from the EAmt are characterized by significant volume percent garnet + clinopyroxene with densities up to 3.5 g/cm<sup>3</sup> and  $V_p = 7.4$  km/s (Figure 14e,f) (Williams et al. 2014). This modeling suggests that some rocks of the EAmt may have been dense enough to founder into the mantle.

Phase equilibria modeling applied to rocks of the EAmt demonstrates that this portion of the Athabasca granulite terrane may be representative of lower continental crust. The EAmt bulk composition falls within the range of lower crustal bulk compositions derived by Hacker et al. (2015; see Figure 1). Seismic velocities and densities of several EAmt rocks are in agreement with those observed for what is a lithologically heterogeneous lower continental crust (Figure 14) (Rudnick & Gao 2014, Hacker et al. 2015).

## Dynamic Rheology of Lower Continental Crust

The rheology of lower continental crust exerts a first-order control on the mechanical behavior of the lithosphere (Jackson 2002, Bürgmann & Dresen 2008, Thatcher & Pollitz 2008). Lower crustal rheology in orogenic zones is arguably dynamic, with periods of weak flow followed by high strength (Klepeis et al. 2003, Dumond et al. 2010). Other regions may be characterized by rheological heterogeneity (Jamieson et al. 2007). As an example, weak lower crustal flow is inferred to underlie much of central and eastern Tibet, coincident with zones of low shear wave velocity (Yao et al. 2010), high conductivity (Bai et al. 2010, Le Pape et al. 2012), and dramatic subhorizontal seismic reflectivity in the deep crust (Ross et al. 2004). Rare sections of exhumed lower continental crust provide important field-based constraints that may be used as analogs for understanding modern orogenic systems like Tibet (e.g., Percival et al. 1992, Klepeis et al. 2007, Dumond et al. 2010, Bonamici et al. 2011). Subhorizontal fabrics exposed in the Mary batholith of the EAmt provide an analog for the nature of lower crustal flow (Figure 7). Dumond et al. (2010) and Regan et al. (2014, 2017b) documented hundreds of square kilometers of penetrative,



(Caption appears on following page)

**Figure 14** (Figure appears on preceding page)

Phase equilibrium diagrams generated with Purple\_X 6.7.7 (Connolly 2005) for felsic and mafic rock compositions from the East Athabasca mylonite triangle in the Athabasca granulite terrane. (a,b) Orthopyroxene-bearing felsic granitoid with an equilibrium assemblage that evolves to Grt + Cpx + Pl + Kfs during isobaric cooling. (a) Phase equilibrium diagram contoured for density. (b) Phase equilibrium diagram contoured for vol% Grt with an isobaric cooling path indicated showing evolution of primary wave (P-wave) velocity in this rock type. (c,d) Garnet-rich residual felsic granulite with an equilibrium assemblage of Bt + Grt + Kfs + Pl + Ky + Rt. The mode of garnet in this field is 28–30 vol%. (c) Phase equilibrium diagram contoured for density indicating a density near  $3.1 \text{ g/cm}^3$  for the felsic granulite. (d) Phase equilibrium diagram contoured for seismic velocity indicating a P-wave velocity near 7.0 km/s for a felsic granulite bulk composition. (e,f) Phase equilibrium diagrams for mafic granulite with the equilibrium assemblage indicated in the white stippled field. (e) Phase equilibrium diagram contoured for density showing a density of  $3.5 \text{ g/cm}^3$  for Grt + Cpx + Pl + Qtz mafic granulite. (f) Phase equilibrium diagram contoured for seismic velocity indicates a P-wave velocity of 7.4 km/s for the mafic granulite. Abbreviations: Bt, biotite; Cpx, clinopyroxene; Grt, garnet; Hb, hornblende; Ilm, ilmenite; Kfs, K-feldspar; Ky, kyanite; L, liquid; Ms, muscovite; Opx, orthopyroxene; Pl, plagioclase; Qtz, quartz; Rt, rutile; Sil, sillimanite.

high-temperature and high-pressure ribbon mylonite fabric with uniform top-to-the-southeast kinematics of flow along subhorizontal fabrics in a heterogeneous suite of rock types, ranging from feldspar porphyroblast-rich orthogneisses to garnet-bearing migmatites (Figure 7). The character and consistent direction of subhorizontal flow are consistent with detachment-style flow above the crust–mantle boundary (Weber 1986, Tikoff et al. 2002, Williams & Jiang 2005). This record of relatively low-viscosity subhorizontal shear strain at >30-km depths implies that stresses were transmitted horizontally through the crust as it was decoupled from the underlying crust and mantle (Royden 1996). This low-viscosity behavior was contemporaneous with dramatic melt weakening in the Upper Deck domain of the EAmt, where felsic granulites document pervasive fluid absent melting of biotite and growth of synkinematic garnet and orthopyroxene coincident with subhorizontal fabric development (Dumond et al. 2015). Syndeformational reactions were important during lower crustal flow and may have facilitated further weakening and strain localization (e.g., Rutter & Brodie 1995, Stünitz & Tullis 2001, Miranda & Klepeis 2016).

The period of Neoarchean lower crustal flow in the EAmt is interpreted to have been followed by a protracted episode of isobaric cooling and lower crustal residence (Williams et al. 2000, Williams & Hanmer 2006, Flowers et al. 2008, Mahan et al. 2008). Penetrative  $D_1$  subhorizontal flow fabrics were overprinted by upright open to tight  $F_2$  folds, rare axial-planar cleavage, discrete zones of steep fabric development, outcrop- to crustal-scale steeply dipping shear zones, and local reactivation and buckling of  $S_1$  fabrics in the Paleoproterozoic. The discrete and highly partitioned character of 1.92–1.90 Ga  $D_2$  strain implies that lower continental crust, as represented by the Mary batholith and Upper Deck domain, had evolved into a lower crustal “strength beam” (i.e., Karlstrom & Williams 1998). Results from the EAmt reveal an important dichotomy that has been documented elsewhere, e.g., the lower arc crust of Fiordland (Klepeis et al. 2003, 2004, 2007). The strength of continental lower crust is dynamic and evolving. Flow of relatively weak lower crust during batholith emplacement and production of subhorizontal fabrics was followed by a period of near-isobaric cooling and strengthening. The character of the strengthened crust influenced subsequent deformation events. Pervasive low-viscosity flow and fabric development at ca. 2.60–2.55 Ga contrasts with the highly partitioned strain and localized shearing on steeply dipping fabrics that occurred at ca. 1.9 Ga (Mahan et al. 2008; Dumond et al. 2010; Bethune et al. 2013; Regan et al. 2014, 2017b). It is noteworthy that despite the influx of heat from the mantle signaled by the Chipman mafic dike swarm at 2.1–1.9 Ga in the adjoining Chipman domain

(Flowers et al. 2006a, Regan et al. 2018), the Mary batholith did not sufficiently weaken to flow or strain in the manner it did previously (except in regions adjacent to the dike swarm). Similar conclusions were drawn for the Western Fiordland Orthogneiss in New Zealand, whereby zones weakened by melt and heat during lower crustal emplacement coincided with subhorizontal flow prior to cooling, strengthening, and steep fabric/shear zone development (Klepeis et al. 2004). We suggest that once strengthened, the deep crust can transmit stresses over long distances, and thus it is possible for tectonic activity to be localized in regions that are hundreds of kilometers from plate boundary activity.

In summary, from a rheological perspective, we infer that the bulk felsic EAmt lower crust was weaker than what would be expected for a more mafic lower crust. Felsic to intermediate bulk compositions and the occurrence of melt both led to dramatic weakening and penetrative flow that would not be expected for more mafic dehydrated bulk compositions. In the absence of fluids, melting, or rehydration, mafic granulite bulk compositions would potentially resist strain localization, with the end result being the partitioning of strain into the weaker felsic bulk compositions. Subsequent rehydration and the introduction of fluids would facilitate strain localization and shear zone development in the strong mafic rocks (e.g., Getsinger et al. 2013).

## Stabilization Versus Destabilization of Continental Lithosphere

Identifying the mechanisms responsible for the stabilization and destabilization of the continents is critical for our understanding of the origin and evolution of cratonic lithosphere (Moyen et al. 2017). Portions of the Athabasca granulite terrane (e.g., the EAmt) represent stabilized continental lithosphere with evidence for long-term lower crustal residence between 2.55 and 1.9 Ga (Williams & Hanmer 2006, Flowers et al. 2008, Mahan et al. 2008). Other parts of the terrane represent regions of short-term (10s to >100 Myr) residence prior to their uplift and exhumation to Earth’s surface (e.g., Snowbird Lake and Beaverlodge domains; Martel et al. 2008, Bethune et al. 2013). The period between 1.9 and 1.7 Ga represents a time of lithospheric reactivation for the entire Athabasca granulite terrane that was followed by a return to cratonic stability signaled by the deposition of the 1.7 Ga Athabasca intracratonic basin (Flowers et al. 2006a,b, 2008; Rainbird et al. 2007).

Mechanisms for stabilization of continental lithosphere include emplacement and subsequent isobaric cooling of felsic to mafic magmas into the lower crust. These are best illustrated by the Mary batholith, the Bohica mafic complex, and felsic and mafic granulite layers throughout the EAmt (Williams et al. 2000; Mahan et al. 2008; Dumond et al. 2010, 2015; Regan et al. 2017b). The emplacement of these rocks was followed by ubiquitous garnet growth, leading to densification and stabilization during subhorizontal fabric development and subsequent isobaric cooling (Williams et al. 2014, Dumond et al. 2015). Reactivation and destabilization of continental lithosphere can be attributed in part to emplacement of mafic magmas and/or fluids associated with asthenospheric upwelling, as represented by the 2.1–1.9 Ga Chipman mafic dike swarm. This allowed the thermally softened Athabasca granulite terrane to experience far-field stresses related to the Taltson orogeny (Regan et al. 2014). Subsequent strain in the Athabasca granulite terrane after 1.9 Ga was localized along steeply dipping fabrics and shear zones, signaling a return to stronger and more stabilized lithosphere.

## DISCLOSURE STATEMENT

The authors are not aware of any affiliations, memberships, funding, or financial holdings that might be perceived as affecting the objectivity of this review.

## ACKNOWLEDGMENTS

This manuscript is based on work supported by National Science Foundation grants EAR-0310004, EAR-0609935, EAR-0816394, EAR-1255277, and EAR-1419843. We appreciate the reviewer's comments, which helped to improve the manuscript.

## LITERATURE CITED

Ansdel KM. 2005. Tectonic evolution of the Manitoba-Saskatchewan segment of the Paleoproterozoic Trans-Hudson orogen, Canada. *Can. J. Earth Sci.* 42:741–59

Ashton KE, Hartlaub RP, Bethune KM, Heaman LM, Rayner N, Niebergall GR. 2013. New depositional age constraints for the Murmac Bay Group of the southern Rae craton, Canada. *Precambrian Res.* 232:70–88

Ashton KE, Hartlaub RP, Heaman LM, Morelli RM, Card CD, et al. 2009. Post-Talton sedimentary and intrusive history of the southern Rae Province along the northern margin of the Athabasca basin, western Canadian Shield. *Precambrian Res.* 175:16–34

Aspler LB, Chiarenzelli JR. 1996. Stratigraphy, sedimentology and physical volcanology of the Henik Group, central Ennadai-Rankin greenstone belt, Northwest Territories, Canada: late Archean paleogeography of the Hearne Province and tectonic implications. *Precambrian Res.* 77:59–89

Aspler LB, Cousens BL, Chiarenzelli JR. 2002. Griffin gabbro sills (2.11 Ga), Hurwitz basin, Nunavut, Canada: long-distance lateral transport of magmas in western Churchill Province crust. *Precambrian Res.* 117:269–94

Bai D, Unsworth MJ, Meju MA, Ma X, Teng J, et al. 2010. Crustal deformation of the eastern Tibetan plateau revealed by magnetotelluric imaging. *Nat. Geosci.* 3:358–62

Baldwin JA, Bowring SA, Williams ML. 2003. Petrological and geochronological constraints on high pressure, high temperature metamorphism in the Snowbird tectonic zone, Canada. *J. Metamorph. Geol.* 21:81–98

Baldwin JA, Bowring SA, Williams ML, Mahan KH. 2006. Geochronological constraints on the evolution of high-pressure felsic granulites from an integrated electron microprobe and ID-TIMS geochemical study. *Lithos* 88:173–200

Baldwin JA, Bowring SA, Williams ML, Williams IS. 2004. Eclogites of the Snowbird tectonic zone: petrological and U-Pb geochronological evidence for Paleoproterozoic high-pressure metamorphism in the western Canadian Shield. *Contrib. Mineral. Petrol.* 147:528–48

Baldwin JA, Powell R, White RW, Stipska P. 2015. Using calculated chemical potential relationships to account for replacement of kyanite by symplectite in high pressure granulites. *J. Metamorph. Geol.* 33:311–30

Baldwin JA, Powell R, Williams ML, Goncalves P. 2007. Formation of eclogite, and reaction during exhumation to mid-crustal levels, Snowbird tectonic zone, western Canadian Shield. *J. Metamorph. Geol.* 25:953–74

Berman RG, Davis WJ, Pehrsson S. 2007. Collisional Snowbird tectonic zone resurrected: growth of Laurentia during the 1.9 Ga accretionary phase of the Hudsonian orogeny. *Geology* 35:911–14

Berman RG, Pehrsson S, Davis WJ, Ryan JJ, Qui H, Ashton KE. 2013. The Arrowsmith orogeny: geochronological and thermobarometric constraints on its extent and tectonic setting in the Rae craton, with implications for pre-Nuna supercontinent reconstruction. *Precambrian Res.* 232:44–69

Berman RG, Sanborn-Barrie M, Stern RA, Carson CJ. 2005. Tectonometamorphism at ca. 2.35 and 1.85 Ga in the Rae domain, western Churchill Province, Nunavut, Canada: insights from structural, metamorphic and in situ geochronological analysis of the southwestern Committee Bay belt. *Can. Mineral.* 43:409–42

Bethune KM, Berman RG, Rayner N, Ashton KE. 2013. Structural, petrological and U-Pb SHRIMP geochronological study of the western Beaverlodge domain: implications for crustal architecture, multi-stage orogenesis and the extent of the Talton orogen in the SW Rae craton, Canadian Shield. *Precambrian Res.* 232:89–118

Bickford ME, Collerson KD, Lewry JF. 1994. Crustal history of the Rae and Hearne Provinces, southwestern Canadian Shield, Saskatchewan: constraints from geochronologic and isotopic data. *Precambrian Res.* 68:1–21

Biermeier C, Wiesinger M, Stuwe K, Foster DA, Gibson HJ, Raza A. 2003. Aspects of the structural and late thermal evolution of the Redbank thrust system, central Australia: constraints from the Spears metamorphics. *Aust. J. Earth Sci.* 50:983–99

Bonamici CE, Tikoff B, Goodwin LB. 2011. Anatomy of a 10 km scale sheath fold, Mount Hay Ridge, Arunta Region, central Australia: the structural record of deep crustal flow. *Tectonics* 30:TC6015

Bucher K, Frey M. 2002. *Petrogenesis of Metamorphic Rocks*. Berlin: Springer

Bürgmann R, Dresen G. 2008. Rheology of the lower crust and upper mantle: evidence from rock mechanics, geodesy, and field observations. *Annu. Rev. Earth Planet. Sci.* 36:531–67

Card CD, Bethune KM, Davis WJ, Rayner N, Ashton KE. 2014. The case for a distinct Taltson orogeny: evidence from northwest Saskatchewan, Canada. *Precambrian Res.* 255:245–65

Card CD, Pana D, Portella P, Thomas DJ, Annesley IR. 2007. Basement rocks to the Athabasca Basin, Saskatchewan and Alberta. In *EXTECH IV: Geology and Uranium Exploration Technology of the Proterozoic Athabasca Basin, Saskatchewan and Alberta*, ed. CW Jefferson, G Delaney, pp. 69–87. Geol. Surv. Can. Bull. 588. Ottawa: Geol. Surv. Can.

Chapman D, Furlong KP. 1992. Thermal state of the continental lower crust. In *Continental Lower Crust*, ed. DM Fountain, R Arculus, RW Kay, pp. 179–99. Dev. Geotecton. 23. Amsterdam: Elsevier

Chiarenzelli J, Aspler L, Villeneuve M, Lewry J. 1998. Early Proterozoic evolution of the Saskatchewan craton and its allochthonous cover, Trans-Hudson orogen. *J. Geol.* 106:247–67

Condie KC. 1993. Chemical composition and evolution of the upper continental crust: contrasting results from surface samples and shales. *Chem. Geol.* 104:1–37

Connolly JAD. 2005. Computation of phase equilibria by linear programming: a tool for geodynamic modeling and its application to subduction zone decarbonation. *Earth Planet. Sci. Lett.* 236:524–41

Connolly JAD, Kerrick DM. 2002. Metamorphic controls on seismic velocity of subducted oceanic crust at 100–250 km depth. *Earth Planet. Sci. Lett.* 204:61–74

Copley A, Avouac JP, Wernicke B. 2011. Evidence for mechanical coupling and strong Indian lower crust beneath southern Tibet. *Nature* 472:79–81

Corrigan D, Pehrsson S, Wodicka N, de Kemp E. 2009. The Paleoproterozoic Trans-Hudson orogen: a prototype of modern accretionary processes. In *Ancient Orogens and Modern Analogues*, ed. JB Murphy, JD Keppe, AJ Hynes, pp. 457–79. London: Geol. Soc. Lond.

Cousens BL, Aspler LB, Chiarenzelli JR, Donaldson JA, Sandeman HA, et al. 2001. Enriched Archean lithospheric mantle beneath western Churchill Province tapped during Paleoproterozoic orogenesis. *Geology* 29:827–30

Currie C, Hyndman R. 2006. The thermal structure of subduction zone back arcs. *J. Geophys. Res.* 111:B08404

Davis WJ, Hanmer S, Tella S, Sandeman HA, Ryan JJ. 2006. U-Pb geochronology of the MacQuoid supracrustal belt and Cross Bay plutonic complex: key components of the northwestern Hearne subdomain, western Churchill Province, Nunavut, Canada. *Precambrian Res.* 145:53–80

Ducea M. 2011. Fingerprinting orogenic delamination. *Geology* 39:191–92

Dumond G, Goncalves P, Williams ML, Jercinovic MJ. 2010. Subhorizontal fabric in exhumed continental lower crust and implications for lower crustal flow: Athabasca granulite terrane, western Canadian Shield. *Tectonics* 29:TC2006

Dumond G, Goncalves P, Williams ML, Jercinovic MJ. 2015. Monazite as a monitor of melting, garnet growth and feldspar recrystallization in continental lower crust. *J. Metamorph. Geol.* 33:735–62

Dumond G, Mahan KH, Williams ML, Jercinovic MJ. 2013. Transpressive uplift and exhumation of continental lower crust revealed by synkinematic monazite reactions. *Lithosphere* 5:507–12

Dumond G, McLean N, Williams ML, Jercinovic MJ, Bowring SA. 2008. High-resolution dating of granite petrogenesis and deformation in a lower crustal shear zone: Athabasca granulite terrane, western Canadian Shield. *Chem. Geol.* 254:175–96

Dumond G, Williams ML, Baldwin JA, Jercinovic MJ. 2017. Backarc origin for Neoarchean ultrahigh-temperature metamorphism, eclogitization, and orogenic root growth. *Geology* 45:943–46

Fahrig WF, Christie KW, Eade KE, Tella S. 1984. Paleomagnetism of the Tulemalu dykes, Northwest Territories, Canada. *Can. J. Earth Sci.* 21:544–53

Fischer KM. 2002. Waning buoyancy in the crustal roots of old mountains. *Nature* 417:933–36

Flowers RM, Bowring S, Mahan KH, Williams ML. 2008. Stabilization and reactivation of cratonic lithosphere from the lower crustal record in the western Canadian Shield. *Contrib. Mineral. Petro.* 156:529–49

Flowers RM, Bowring SA, Williams ML. 2006a. Timescales and significance of high-pressure, high-temperature metamorphism and mafic dike anatexis, Snowbird tectonic zone, Canada. *Contrib. Mineral. Petro.* 151:558–81

Flowers RM, Mahan KH, Bowring SA, Williams ML, Pringle MS, Hodges KV. 2006b. Multistage exhumation and juxtaposition of lower continental crust in the western Canadian Shield: linking high-resolution U-Pb and  $^{40}\text{Ar}/^{39}\text{Ar}$  thermochronometry with pressure-temperature-deformation paths. *Tectonics* 25:TC4003

Fountain DM, Salisbury MH. 1981. Exposed cross-sections through continental crust: implications for crustal structure, petrology and evolution. *Earth Planet. Sci. Lett.* 5:263–77

Getsinger AJ, Hirth G, Stunitz H, Goergen ET. 2013. Influence of water on rheology and strain localization in the lower continental crust. *Geochim. Geophys. Geosyst.* 14:2247–64

Gibb RA, Thomas MD, Lapointe PL, Mukhopadhyay M. 1983. Geophysics of proposed Proterozoic sutures in Canada. *Precambrian Res.* 19:349–84

Green DH, Hibberson WO, Rosenthal A, Kovács I, Yaxley GM, et al. 2014. Experimental study of the influence of water on melting and phase assemblages in the upper mantle. *J. Petrol.* 55:2067–96

Green DH, Ringwood AE. 1967. An experimental investigation of the gabbro to eclogite transformation and its petrological applications. *Geochim. Cosmochim. Acta* 31:767–833

Hacker BR, Abers GA. 2004. Subduction Factory 3: an Excel worksheet and macro for calculating the densities, seismic wave speeds, and  $\text{H}_2\text{O}$  contents of minerals and rocks at pressure and temperature. *Geochim. Geophys. Geosyst.* 5:Q01005

Hacker BR, Gnos E, Ratschbacher L, Grove M, McWilliams M, et al. 2000. Hot and dry deep crustal xenoliths from Tibet. *Science* 287:2463–66

Hacker BR, Kelemen PB, Behn MD. 2011. Differentiation of the continental crust by relamination. *Earth Planet. Sci. Lett.* 307:501–16

Hacker BR, Kelemen PB, Behn MD. 2015. Continental lower crust. *Annu. Rev. Earth Planet. Sci.* 43:167–205

Hacker BR, Ritzwoller MH, Xie J. 2014. Partially melted, mica-bearing crust in Central Tibet. *Tectonics* 33:1408–24

Hajnal Z, Lewry J, White D, Ashton K, Clowes R, et al. 2005. The Sask craton and Hearne Province margin: seismic reflection studies in the western Trans-Hudson orogen. *Can. J. Earth Sci.* 42:403–19

Hanmer S. 1994. *Geology, East Athabasca mylonite triangle, Saskatchewan*. Map 1859A, Scale 1:100000, Geol. Surv. Can., Ottawa

Hanmer S. 1997. *Geology of the Striding-Athabasca Mylonite Zone, Northern Saskatchewan and Southeastern District of Mackenzie, Northwest Territories*. Geol. Surv. Can Bull. 501. Ottawa: Geol. Surv. Can.

Hanmer S, Bowring SA, Van Breeman O, Parrish RR. 1992. Great Slave Lake shear zone, northwest Canada: mylonitic record of Early Proterozoic convergence, collision, and indentation. *J. Struct. Geol.* 14:757–73

Hanmer S, Parrish RR, Williams ML, Kopf C. 1994. Striding-Athabasca mylonite zone: complex Archean deep crustal deformation in the East Athabasca mylonite triangle, N. Saskatchewan. *Can. J. Earth Sci.* 31:1287–300

Hanmer S, Sandeman HA, Davis WJ, Aspler LB, Rainbird RH, et al. 2004. Geology and Neoarchean tectonic setting of the central Hearne supracrustal belt, Western Churchill Province, Nunavut, Canada. *Precambrian Res.* 134:63–83

Hanmer S, Tella S, Ryan JJ, Sandeman HA, Berman RG. 2006. Late Neoarchean thick-skinned thrusting and Paleoproterozoic reworking in the MacQuoid supracrustal belt and Cross Bay plutonic complex, western Churchill Province, Nunavut, Canada. *Precambrian Res.* 144:126–39

Hanmer S, Williams ML. 2001. *Targeted fieldwork in the Daly Bay complex, Hudson Bay, Nunavut*. Curr. Res. 2001-C15, Geol. Surv. Can., Ottawa

Hanmer S, Williams ML, Kopf C. 1995. Modest movements, spectacular fabrics in an intracontinental deep-crustal strike-slip fault: Striding-Athabasca mylonite zone, NW Canadian Shield. *J. Struct. Geol.* 17:493–507

Hartlaub RP, Chacko T, Heaman LM, Creaser RA, Ashton KE, Simonetti A. 2005. Ancient (Meso- to Paleoproterozoic) crust in the Rae Province, Canada: evidence from Sm-Nd and U-Pb constraints. *Precambrian Res.* 141:137–53

Hartlaub RP, Heaman LM, Chacko T, Ashton KE. 2007. Circa 2.3-Ga magmatism of the Arrowsmith orogeny, Uranium City region, western Churchill craton, Canada. *J. Geol.* 115:181–95

Hildebrand RS, Hoffman PF, Bowring SA. 2010. The Calderian orogeny in Wopmay orogen (1.9 Ga), northwestern Canadian Shield. *Geol. Soc. Am. Bull.* 122:794–814

Hoffman PF. 1987. Continental transform tectonics; Great Slave Lake shear zone (ca. 1.9 Ga), Northwest Canada. *Geology* 15:785–88

Hoffman PF. 1988. United Plates of America, the birth of a craton: early Proterozoic assembly and growth of Laurentia. *Annu. Rev. Earth Planet. Sci.* 16:543–603

Holland TJB, Powell R. 1998. An internally consistent thermodynamic data set for phases of petrological interest. *J. Metamorph. Geol.* 16:309–43

Huang Y, Chubakov V, Mantovani F, Rudnick RL, McDonough WF. 2013. A reference Earth model for the heat-producing elements and associated geoneutrino flux. *Geochem. Geophys. Geosyst.* 14:2003–29

Jackson J. 2002. Strength of the continental lithosphere: time to abandon the jelly sandwich? *GSA Today* 12:4–10

Jamieson RA, Beaumont C, Nguyen MH, Culshaw NG. 2007. Synconvergent ductile flow in variable-strength continental crust: numerical models with application to the western Grenville orogen. *Tectonics* 26:TC5005

Jones AG, Snyder D, Hanmer S, Asudeh I, White D, et al. 2002. Magnetotelluric and teleseismic study across the Snowbird tectonic zone, Canadian Shield: A Neoarchean mantle suture? *Geophys. Res. Lett.* 29:1829

Karlstrom KE, Williams ML. 1998. Heterogeneity of the middle crust: implications for strength of continental lithosphere. *Geology* 26:815–18

Kelemen PB, Hanghoj K, Greene AR. 2003. One view of the geochemistry of subduction-related magmatic arcs, with an emphasis on primitive andesite and lower crust. In *Treatise on Geochemistry*, Vol. 3: The Crust, ed. RL Rudnick, pp. 593–659. Oxford, UK: Elsevier-Pergamon. 1st ed.

Klepeis KA, Clarke GL, Gehrels G, Vervoort J. 2004. Processes controlling vertical coupling and decoupling between the upper and lower crust of orogens: results from Fiordland, New Zealand. *J. Struct. Geol.* 26:765–91

Klepeis KA, Clarke GL, Rushmer T. 2003. Magma transport and coupling between deformation and magmatism in the continental lithosphere. *GSA Today* 13:4–11

Klepeis KA, King D, De Paoli M, Clarke GL, Gehrels G. 2007. Interaction of strong lower and weak middle crust during lithospheric extension in western New Zealand. *Tectonics* 26:TC4017

Kopf CF. 1999. *Deformation, metamorphism, and magmatism in the East Athabasca mylonite triangle, northern Saskatchewan: implications for the Archean and Early Proterozoic crustal structure of the Canadian Shield*. PhD Thesis, Dep. Geosci., Univ. Mass., Amherst

Koteas GC, Williams ML, Seaman SJ, Dumond G. 2010. Granite genesis and mafic-felsic magma interaction in the lower crust. *Geology* 38:1067–70

Krikorian L. 2002. *Geology of the Wholdaia Lake segment of the Snowbird tectonic zone, Northwest Territories (Nunavut): a view of the deep crust during assembly and stabilization of the Laurentian craton*. Master's Thesis, Dep. Geosci., Univ. Mass., Amherst

Le Pape F, Jones AG, Vozar J, Wenbo W. 2012. Penetration of crustal melt beyond the Kunlun Fault into northern Tibet. *Nat. Geosci.* 5:330–35

Macdonald R. 1980. New edition of the geological map of Saskatchewan, Precambrian Shield area. *Summ. Investig. Sask. Geol. Surv.* 1980:19–21

MacLachlan K, Davis WJ, Relf C. 2005a. Paleoproterozoic reworking of an Archean thrust fault in the Hearne domain, Western Churchill Province: U-Pb geochronological constraints. *Can. J. Earth Sci.* 42:1313–30

MacLachlan K, Davis WJ, Relf C. 2005b. U/Pb geochronological constraints on Neoarchean tectonism: multiple compressional events in the northwestern Hearne domain, Western Churchill Province, Canada. *Can. J. Earth Sci.* 42:85–109

Mahan KH, Goncalves P, Flowers R, Williams ML, Hoffman-Setka D. 2008. The role of heterogeneous strain in the development and preservation of a polymetamorphic record in high-P granulites, western Canadian Shield. *J. Metamorph. Geol.* 26:669–94

Mahan KH, Goncalves P, Williams ML, Jercinovic MJ. 2006a. Dating metamorphic reactions and fluid flow: application to exhumation of high-P granulites in a crustal-scale shear zone, western Canadian Shield. *J. Metamorph. Geol.* 24:193–217

Mahan KH, Schulte-Pelkum V, Blackburn TJ, Bowring SA, Dudas FO. 2012. Seismic structure and lithospheric rheology from deep crustal xenoliths, central Montana, USA. *Geochem. Geophys. Geosyst.* 13:1–11

Mahan KH, Smit A, Williams ML, Dumond G, Van Reenen DD. 2011. Heterogeneous strain and polymetamorphism in high-grade terranes: insight into crustal processes from the Athabasca granulite terrane, western Canada and Limpopo complex, southern Africa. In *Origin and Evolution of Precambrian High-Grade Gneiss Terranes, with Special Emphasis on the Limpopo Complex of Southern Africa*, ed. S McCourt, J Kramers, DD Van Reenen, pp. 269–87. Boulder, CO: Geol. Soc. Am.

Mahan KH, Williams ML. 2005. Reconstruction of a large deep-crustal terrane: implications for the Snowbird tectonic zone and early growth of Laurentia. *Geology* 33:385–88

Mahan KH, Williams ML, Baldwin JA. 2003. Contractional uplift of deep crustal rocks along the Legs Lake shear zone, western Churchill Province, Canadian Shield. *Can. J. Earth Sci.* 40:1085–110

Mahan KH, Williams ML, Flowers RM, Jercinovic MJ, Baldwin JA, Bowring SA. 2006b. Geochronological constraints on the Legs Lake shear zone with implications for regional exhumation of lower continental crust, western Churchill Province, Canadian Shield. *Contrib. Mineral. Petrol.* 152:223–42

Martel E, van Breemen O, Berman RG, Pehrsson S. 2008. Geochronology and tectonometamorphic history of the Snowbird Lake area, Northwest Territories, Canada: new insights into the architecture and significance of the Snowbird tectonic zone. *Precambrian Res.* 161:201–30

Massonne HJ, Willner A, Gerya T. 2007. Densities of metapelitic rocks at high to ultrahigh pressure conditions: What are the geodynamic consequences? *Earth Planet. Sci. Lett.* 256:12–27

McDonough MR, McNicoll VJ, Schetselaar EM, Grover TW. 2000. Geochronological and kinematic constraints on crustal shortening and escape in a two-sided oblique-slip collisional and magmatic orogen, Paleoproterozoic Talton magmatic zone, northeastern Alberta. *Can. J. Earth Sci.* 37:1549–73

McDonough WF, Sun SS. 1995. The composition of the Earth. *Chem. Geol.* 120:223–53

Mills AJ, Berman RG, Davis WJ, Tella S, Carr S, et al. 2007. Thermobarometry and geochronology of the Uvauk complex, a polymetamorphic Neoarchean and Paleoproterozoic segment of the Snowbird tectonic zone, Nunavut, Canada. *Can. J. Earth Sci.* 44:245–66

Miranda EA, Kleipeis K. 2016. The interplay and effects of deformation and crystallized melt on the rheology of the lower continental crust, Fiordland, New Zealand. *J. Struct. Geol.* 93:91–105

Moyen JF, Paquette JL, Ionov DA, Gannoun A, Korsakov AV, et al. 2017. Paleoproterozoic rejuvenation and replacement of Archean lithosphere: evidence from zircon U-Pb dating and Hf isotopes in crustal xenoliths at Udachnaya, Siberian craton. *Earth Planet. Sci. Lett.* 457:149–59

Ohno I, Harada K, Yoshitomi C. 2006. Temperature variation of elastic constants of quartz across the  $\alpha$ - $\beta$  transition. *Phys. Chem. Miner.* 33:1–9

Pehrsson SJ, Berman RG, Eglington BM, Rainbird RH. 2013. Two Neoarchean supercontinents revisited: the case for a Rae family of cratons. *Precambrian Res.* 232:27–43

Percival JA, Fountain DM, Salisbury MH. 1992. Exposed crustal cross sections as windows on the lower crust. In *Continental Lower Crust*, ed. DM Fountain, R Arculus, RW Kay, pp. 317–62. Amsterdam: Elsevier

Percival JA, West GF. 1994. The Kapuskasing uplift: a geological and geophysical synthesis. *Can. J. Earth Sci.* 31:1256–86

Rainbird RH, Stern RA, Rayner N, Jefferson CW. 2007. Age, provenance, and regional correlation of the Athabasca Group, Saskatchewan and Alberta, constrained by igneous and detrital zircon geochronology. In *EXTECH IV: Geology and Uranium Exploration Technology of the Proterozoic Athabasca Basin, Saskatchewan and Alberta*, ed. CW Jefferson, G Delaney, pp. 193–209. Geol. Surv. Can. Bull. 599. Ottawa: Geol. Surv. Can.

Regan SP, Williams ML, Chiarenzelli JR, Grohn L, Mahan KH, Gallagher M. 2017a. Isotopic evidence for Neoarchean continuity across the Snowbird tectonic zone, western Churchill Province, Canada. *Precambrian Res.* 300:201–22

Regan SP, Williams ML, Grohn L, Chiarenzelli JR, Jercinovic MJ, et al. 2018. Evidence for an aborted rift origin for the central Snowbird tectonic zone, Canada. In review

Regan SP, Williams ML, Leslie S, Mahan KH, Jercinovic MJ, Holland ME. 2014. The Cora Lake shear zone, Athabasca granulite terrane, an intraplate response to far-field orogenic processes during the amalgamation of Laurentia. *Can. J. Earth Sci.* 51:877–901

Regan SP, Williams ML, Mahan KH, Dumond G, Jercinovic MJ, Orlandini OF. 2017b. Neoarchean arc magmatism and subsequent collisional orogenesis along the eastern Rae domain, western Churchill Province: implications for the early growth of Laurentia. *Precambrian Res.* 294:151–74

Ross AR, Brown LD, Pananont P, Nelson KD, Klemperer S, et al. 2004. Deep reflection surveying in central Tibet: lower-crustal layering and crustal flow. *Geophys. J. Int.* 156:115–28

Ross GM. 2002. Evolution of Precambrian continental lithosphere in Western Canada: results from Lithoprobe studies in Alberta and beyond. *Can. J. Earth Sci.* 39:413–37

Royden L. 1996. Coupling and decoupling of crust and mantle in convergent orogens: implications for strain partitioning in the crust. *J. Geophys. Res.* 101:17679–705

Rudnick RL. 1992. Restites, Eu anomalies, and the lower continental crust. *Geochim. Cosmochim. Acta* 56:963–70

Rudnick RL, Fountain DM. 1995. Nature and composition of the continental crust: a lower crustal perspective. *Rev. Geophys.* 33:267–309

Rudnick RL, Gao S. 2003. Composition of the continental crust. In *Treatise on Geochemistry*, Vol. 3: The Crust, ed. RL Rudnick, pp. 1–64. Oxford, UK: Elsevier-Pergamon. 1st ed.

Rudnick RL, Gao S. 2014. Composition of the continental crust. In *Treatise on Geochemistry*, Vol. 4: The Crust, ed. RL Rudnick, pp. 1–51. Oxford, UK: Elsevier-Pergamon. 2nd ed.

Rudnick RL, Presper T. 1990. Geochemistry of intermediate- to high-pressure granulites. In *Granulites and Crustal Evolution*, ed. D Vielzeuf, P Vidal, pp. 523–50. Dordrecht, Neth.: Springer

Rudnick RL, Taylor SR. 1987. The composition and petrogenesis of the lower crust—a xenolith study. *J. Geophys. Res.* 92:13981–4005

Rutter EH, Brodie KH. 1995. Mechanistic interactions between deformation and metamorphism. *Geol. J.* 30:227–40

Sanborn-Barrie M, Carr SD, Thériault R. 2001. Geochronological constraints on metamorphism, magmatism and exhumation of deep-crustal rocks of the Kramanituar complex, with implications for the Paleoproterozoic evolution of the Archean western Churchill Province, Canada. *Contrib. Mineral. Petrol.* 141:592–612

Schulmann K, Kröner A, Hegner E, Wendt I, Konopasek J, et al. 2005. Chronological constraints on the pre-orogenic history, burial and exhumation of deep-seated rocks along the eastern margin of the Variscan orogen, Bohemian Massif, Czech Republic. *Am. J. Sci.* 305:407–48

Schulte-Pelkum V, Mahan KH, Shen W, Stachnik JC. 2017. The distribution and composition of high-velocity lower crust across the continental U.S.: comparison of seismic and xenolith data and implications for lithospheric dynamics and history. *Tectonics* 36:1455–96

Shiels C, Partin CA, Eglington BM. 2016. Provenance approaches in polydeformed metasedimentary successions: determining nearest neighboring cratons during the deposition of the Paleoproterozoic Murmac Bay Group. *Lithosphere* 8:519–32

Slimmon WL. 1989. *Bedrock compilation geology—Fond du Lac (NTS 74-O)*. Map 247A, Scale 1:250000, Sask. Geol. Surv., Sask. Energy Mines, Regina

Slimmon WL, Macdonald R. 1987. Bedrock geological mapping, Pine Channel area (Part of NTS 74O-7 and -8). *Summ. Investig. Sask. Geol. Surv.* 1987:24–33

Snoeyenbos DR, Williams ML, Hamner S. 1995. Archean high-pressure metamorphism in the western Canadian Shield. *Eur. J. Mineral.* 7:1251–72

Stern RA, Berman RG. 2001. Monazite U-Pb and Th-Pb geochronology by ion microprobe, with an application to in situ dating of an Archean metasedimentary rock. *Chem. Geol.* 172:113–30

Stern RA, Card CD, Pana D, Rayner N. 2003. *SHRIMP U-Pb ages of granitoid basement rocks of the southwestern part of the Athabasca Basin, Saskatchewan and Alberta*. Curr. Res. 2003–F3, Geol. Surv. Can., Ottawa

St-Onge MR, Searle MP, Wodicka N. 2006. Trans-Hudson orogen of North America and Himalaya-Karakoram-Tibetan orogen of Asia: structural and thermal characteristics of the lower and upper plates. *Tectonics* 25:TC4006

Stünitz H, Tullis J. 2001. Weakening and strain localization produced by syn-deformational reaction of plagioclase. *Int. J. Earth Sci.* 90:136–48

Tella S, Eade KE. 1986. Occurrence and possible tectonic significance of high-pressure granulite fragments in the Tulemalu fault zone, District of Keewatin, N.W.T., Canada. *Can. J. Earth Sci.* 23:1950–62

Tella S, Hanmer S, Ryan JJ, Sandeman HA, Davis WJ, et al. 2000. 1:100000 scale bedrock geology compilation map of the MacQuoid Lake–Gibson Lake–Cross Bay–Akunak Bay region, western Churchill Province, Nunavut, Canada. *Geol. Assoc. Can. Mineral. Assoc. Can. Program Abstr.* 25. Abstr. 676

Teyssier C. 1985. A crustal thrust system in an intra-cratonic environment. *J. Struct. Geol.* 7:689–700

Thatcher W, Pollitz FF. 2008. Temporal evolution of continental lithospheric strength in actively deforming regions. *GSA Today* 18:4–11

Thompson AB, Schulmann K, Jezek J, Tolar V. 2001. Thermally softened continental zones (arcs and rifts) as precursors to thickened orogenic belts. *Tectonophysics* 332:115–41

Tikoff B, Teyssier C, Waters C. 2002. Clutch tectonics and the partial attachment of lithospheric layers. In *Continental Collision and the Tectono-Sedimentary Evolution of Forelands*, ed. G Bertotti, K Schulmann, SAPL Cloetingh, pp. 57–73. Katlenburg-Lindau, Ger.: Eur. Geophys. U.

van Breeman O, Harper CT, Berman RG, Wodicka N. 2007a. Crustal evolution and Neoarchean assembly of the central-southern Hearne domains: evidence from U-Pb geochronology and Sm-Nd isotopes of the Phelps Lake area, northeastern Saskatchewan. *Precambrian Res.* 159:33–59

van Breeman O, Pehrsson S, Peterson TD. 2007b. *Reconnaissance U-Pb SHRIMP geochronology and Sm-Nd isotope analyses from the Tchery-Wager Bay gneiss domain, western Churchill Province, Nunavut*. Curr. Res. 2007-F2, Geol. Surv. Can., Ottawa

Vielzeuf D, Montel JM. 1994. Partial melting of metagreywackes. Part I. Fluid-absent experiments and phase relationships. *Contrib. Mineral. Petrol.* 117:375–93

Vielzeuf D, Schmidt MW. 2001. Melting relations in hydrous systems revisited: application to metapelites, metagreywackes and metabasalts. *Contrib. Mineral. Petrol.* 141:251–67

Villaseca C, Downes H, Pin C, Barbero L. 1999. Nature and composition of the lower continental crust in central Spain and the Granulite–granite linkage: inferences from granulitic xenoliths. *J. Petrol.* 40:1465–96

Walcott RI. 1968. *The gravity field of northern Saskatchewan and northeastern Alberta with maps*, Gravity Map Ser. 16–20, Earth Phys. Branch, Geol. Surv. Can., Ottawa

Walcott RI, Boyd JB. 1971. *The gravity field of northern Alberta and part of the Northwest Territories and Saskatchewan*. Gravity Map Ser. 103–11. Earth Phys. Branch, Geol. Surv. Can., Ottawa

Wallis RH. 1970. A geological interpretation of gravity and magnetic data, northwest Saskatchewan. *Can. J. Earth Sci.* 7:858–68

Waters-Tormey C, Goodwin LB, Tikoff B, Staffier K, Kelso P. 2009. A granulite facies normal shear zone exposed in the Arunta Inlier of central Australia: implications for deep crustal deformation during oblique divergence. In *Crustal Cross Sections from the Western North American Cordillera and Elsewhere: Implications for Tectonic and Petrologic Processes*, ed. RB Miller, AW Snook, pp. 267–86. Geol. Soc. Am. Spec. Pap. 456. Boulder, CO: Geol. Soc. Am.

Weber K. 1986. Metamorphism and crustal rheology—implications for the structural development of the continental crust during prograde metamorphism. In *The Nature of Lower Continental Crust*, ed. JB Dawson, DA Carswell, J Hall, KH Wedepohl, pp. 95–106. Geol. Soc. Lond. Spec. Publ. 24. London: Geol. Soc. Lond.

Williams ML, Dumond G, Mahan KH, Regan SP, Holland ME. 2014. Garnet-forming reactions in felsic orthogneiss: implications for densification and strengthening of the lower continental crust. *Earth Planet. Sci. Lett.* 405:207–19

Williams ML, Hanmer S. 2006. Structural and metamorphic processes in the lower crust: evidence from a deep-crustal isobarically cooled terrane, Canada. In *Evolution and Differentiation of the Continental Crust*, ed. M Brown, T Rushmer, pp. 231–67. Cambridge, UK: Cambridge Univ. Press

Williams ML, Hamner S, Kopf C, Darrach M. 1995. Syntectonic generation and segregation of tonalitic melts from amphibolite dikes in the lower crust, Striding-Athabasca mylonite zone, northern Saskatchewan. *J. Geophys. Res.* 100:15717–34

Williams ML, Jercinovic MJ. 2002. Microprobe monazite geochronology: putting absolute time into microstructural analysis. *J. Struct. Geol.* 24:1013–28

Williams ML, Karlstrom KE, Dumond G, Mahan KH. 2009. Perspectives on the architecture of continental crust from integrated field studies of exposed isobaric sections. In *Crustal Cross Sections from the Western North American Cordillera and Elsewhere: Implications for Tectonic and Petrologic Processes*, ed. RB Miller, AW Snoke, pp. 219–41. Geol. Soc. Am. Spec. Pap. 456. Boulder, CO: Geol. Soc. Am.

Williams ML, Melis EA, Kopf C, Hamner S. 2000. Microstructural tectonometamorphic processes and the development of gneissic layering: a mechanism for metamorphic segregation. *J. Metamorph. Geol.* 18:41–57

Williams PF, Jiang DZ. 2005. An investigation of lower crustal deformation: evidence for channel flow and its implications for tectonics and structural studies. *J. Struct. Geol.* 27:1486–504

Yao H, van der Hilst RD, Montagner JP. 2010. Heterogeneity and anisotropy of the lithosphere of SE Tibet from surface wave array tomography. *J. Geophys. Res.* 115:B12307

## Contents

A Geologist Reflects on a Long Career <i>Dan McKenzie</i> .....	1
Low-Temperature Alteration of the Seafloor: Impacts on Ocean Chemistry <i>Laurence A. Coogan and Kathryn M. Gillis</i> .....	21
The Thermal Conductivity of Earth's Core: A Key Geophysical Parameter's Constraints and Uncertainties <i>Q. Williams</i> .....	47
Fluids of the Lower Crust: Deep Is Different <i>Craig E. Manning</i> .....	67
Commercial Satellite Imagery Analysis for Countering Nuclear Proliferation <i>David Albright, Sarah Burkhard, and Allison Lach</i> .....	99
Controls on O <sub>2</sub> Production in Cyanobacterial Mats and Implications for Earth's Oxygenation <i>Gregory J. Dick, Sharon L. Grim, and Judith M. Klatt</i> .....	123
Induced Seismicity <i>Katie M. Keranen and Matthew Weingarten</i> .....	149
Superrotation on Venus, on Titan, and Elsewhere <i>Peter L. Read and Sébastien Lebonnois</i> .....	175
The Origin and Evolutionary Biology of Pinnipeds: Seals, Sea Lions, and Walruses <i>Annalisa Berta, Morgan Churchill, and Robert W. Boessenecker</i> .....	203
Paleobiology of Pleistocene Proboscideans <i>Daniel C. Fisher</i> .....	229
Subduction Orogeny and the Late Cenozoic Evolution of the Mediterranean Arcs <i>Leigh Royden and Claudio Faccenna</i> .....	261
The Tasmanides: Phanerozoic Tectonic Evolution of Eastern Australia <i>Gideon Rosenbaum</i> .....	291

Atlantic-Pacific Asymmetry in Deep Water Formation <i>David Ferreira, Paola Cessi, Helen K. Coxall, Agatha de Boer, Henk A. Dijkstra, Sybren S. Drijfhout, Tor Eldevik, Nili Harnik, Jerry F. McManus, David P. Marshall, Johan Nilsson, Fabien Roquet, Tapio Schneider, and Robert C. Wills</i> .....	327
The Athabasca Granulite Terrane and Evidence for Dynamic Behavior of Lower Continental Crust <i>Gregory Dumond, Michael L. Williams, and Sean P. Regan</i> .....	353
Physics of Earthquake Disaster: From Crustal Rupture to Building Collapse <i>Koji Uenishi</i> .....	387
Time Not Our Time: Physical Controls on the Preservation and Measurement of Geologic Time <i>Chris Paola, Vamsi Ganti, David Mohrig, Anthony C. Runkel, and Kyle M. Straub</i> .....	409
The Tectonics of the Altaids: Crustal Growth During the Construction of the Continental Lithosphere of Central Asia Between $\sim$ 750 and $\sim$ 130 Ma Ago <i>A.M. Celâl Şengör, Boris A. Natal'in, Gürsel Sunal, and Rob van der Voo</i> .....	439
The Evolution and Fossil History of Sensory Perception in Amniote Vertebrates <i>Johannes Müller, Constanze Bickelmann, and Gabriela Sobral</i> .....	495
Role of Soil Erosion in Biogeochemical Cycling of Essential Elements: Carbon, Nitrogen, and Phosphorus <i>Asmeret Asefaw Berhe, Rebecca T. Barnes, Johan Six, and Erika Marín-Spiotta</i> .....	521
Responses of the Tropical Atmospheric Circulation to Climate Change and Connection to the Hydrological Cycle <i>Jian Ma, Robin Chadwick, Kyong-Hwan Seo, Changming Dong, Gang Huang, Gregory R. Foltz, and Jonathan H. Jiang</i> .....	549

## Errata

An online log of corrections to *Annual Review of Earth and Planetary Sciences* articles  
may be found at <http://www.annualreviews.org/errata/earth>